

COMPUTER ANALYSIS OF GASTRODUODENAL
ELECTRICAL AND MECHANICAL SIGNALS.



COMPUTER ANALYSIS OF GASTRODUODENAL
ELECTRICAL AND MECHANICAL SIGNALS

by

K. MUNIAPPAN, B.E., M.E.

A Thesis

Submitted to the Faculty of Graduate Studies

in Partial Fulfillment of the Requirements

for the Degree

Master of Engineering

McMaster University

i

MASTER OF ENGINEERING (1976)
(Electrical Engineering)

McMASTER UNIVERSITY
Hamilton, Canada

TITLE: Computer Analysis of Gastroduodenal Electrical and Mechanical
Signals

AUTHOR: K. Muniappan, B.E. (Madras, 1966), M.E. (I.I.Sc., 1969)

SUPERVISORS: Drs. R. Kitai and S.K. Sarna

NUMBER OF PAGES: x, 63

ACKNOWLEDGEMENTS

I would like to thank Professors R. Kitai and S.K. Sarna for their constant encouragement and assistance during the course of this work and in the preparation of the thesis.

I wish to express my thanks to L. Marzio and T.L. Kung for their assistance and discussions and P. Dillon who typed the thesis.

ABSTRACT

The gastroduodenal junction coordination was studied by conducting experiments on six dogs. The electrical and mechanical signals in the gastroduodenal area were recorded by surgically implanting electrodes and strain gauges. Recordings were made on an analog tape recorder for about 30 minutes in the fasted state and for about 45 minutes after food or with intravenous infusion of pentagastrin. The recorded signals were later fed into Data General Nova 830 Minicomputer for subsequent analysis. In analysing these signals frequency is of prime importance as interaction could result in the agumentation of the proximal duodenal electrical/mechanical signal at antral frequency. The application of spectral analysis techniques for this purpose is described.

The programs are developed for the following purposes:

- 1) To accept the analog data and convert them into discrete digital data.
- 2) To display any segment of data for visual observation of recorded signals.
- 3) To compute the auto and cross power spectral density.

The results of the analysis are presented in the form of tables. It is concluded that there exists a coordination. The possible mechanism could be myogenic, since coordination in the electrical activity is evident when atropine was given.

TABLE OF CONTENTS

	<u>PAGE</u>
CHAPTER 1: INTRODUCTION	1
1.1 Intrinsic control mechanisms	1
1.2 Extrinsic control mechanisms	5
1.3 Control loop for gastric emptying	5
CHAPTER 2: METHODS	
2.1 Methods	11
2.2 Measurement of Electrical activity	11
2.3 Measurement of Mechanical activity	13
2.4 Experiments	14
2.5 Computer analysis of Signals.	15
2.5.1 Data Acquisition	18
2.5.2 Display of data	19
2.5.3 Computation of Auto power spectral density	21
2.5.4 Computation of cross spectral density	27
CHAPTER 3: RESULTS	30
CHAPTER 4: CONCLUSIONS	57
BIBLIOGRAPHY	61

LIST OF ILLUSTRATIONS

<u>Figure</u>	<u>Title</u>	<u>Page</u>
1.1	Functional subdivisions of Stomach	2
1.2	Electrical activity recorded from an anaesthetized dog	4
1.3	A feedback control system for gastric emptying	6
2.1	Position of implanted electrodes and strain gauges	12
2.2	Digital signal processing facilities	16
2.3	Schematic diagram of analysis programs	17
2.4	Flow-chart for data acquisition program	20
2.5	Flow-chart for the display of array of points on the graphic terminals	22
2.6	Flow-chart for the computation of auto power spectral density	26
2.7	Flow-chart for cross spectral density computation	29
3.1	Electrical and mechanical activities recorded from a dog (fasted state)	33
3.2	Power spectral density of the pyloric electrical activity - fasted state	34
3.3	Power spectral density of the duodenal electrical activity - fasted state	35
3.4	Electrical and mechanical activities recorded from a dog - 10 minutes after feeding	36

<u>Figure</u>	<u>Title</u>	<u>Page</u>
3.5	Power spectral density of the pyloric electrical activity - 10 minutes after feeding	37
3.6	Power spectral density of the duodenal electrical activity - 10 minutes after feeding	38
3.7	Power spectral density of the pyloric mechanical activity - 10 minutes after feeding	39
3.8	Power spectral density of the duodenal mechanical activity - 10 minutes after feeding	40
3.9	Electrical and mechanical activities recorded from a dog - 4 minutes after pentagastrin	41
3.10	Power spectral density of the pyloric electrical activity - 4 minutes after pentagastrin	42
3.11	Power spectral density of the duodenal electrical activity - 4 minutes after pentagastrin	43
3.12	Power spectral density of the pyloric mechanical activity - 4 minutes after pentagastrin	44
3.13	Power spectral density of the duodenal mechanical activity - 4 minutes after pentagastrin	45
3.14	Electrical and Mechanical activities recorded from a dog - after atropine	46
3.15	Power spectral density of the duodenal electrical activity after atropine	47

LIST OF TABLES

<u>Table</u>	<u>Title</u>	<u>Page</u>
3.1	Results of experiments on Dog no. 1 with feeding	48
3.2	Results of experiments on Dog no. 2 with feeding	49
3.3	Results of experiments on Dog no. 3 with feeding	50
3.4	Results of experiments on Dog no. 4 with feeding	51
3.5	Results of experiments on Dog no. 5 with feeding	52
3.6	Results of experiments on Dog no. 1 with pentagastrin infusion	53
3.7	Results of experiments on Dog no. 2 with pentagastrin infusion	54
3.8	Results of experiments on Dog no. 4 with pentagastrin infusion	55
3.9	Results of experiments on Dog no. 5 with pentagastrin infusion	56

LIST OF SYMBOLS AND ABBREVIATIONS

Ach	Acetylcholine
D	Data offset
EA	Electrode implanted in the antrum
ECA	Electrical control activity
ED	Electrode implanted in the duodenum
EP	Electrode implanted in the pylorus
ERA	Electrical response activity
fs	Sampling frequency
k	No. of subsequences analysed
n	nth sampling instant
N	no. of data points
SGA	Strain gauge implanted in the antrum
SGD	Strain gauge implanted in the duodenum
SGP	Strain gauge implanted in the pylorus
$S_N(w)$	Spectral density at angular frequency w computed from N data points
$S_{xy}(w)$	Cross spectral density of two signals x and y at angular frequency w
x_n	Sampled value of signal x at n th instant
$X_N(w)$	Discrete Fourier coefficient of signal x at angular frequency w
y_n	Sampled value of signal y at n th instant
$Y_N(w)$	Discrete Fourier coefficient of signal y at angular frequency w

LIST OF SYMBOLS AND ABBREVIATIONS

Δf	Resolution in frequency
$\phi_{xy}(w)$	Phase angle of the cross spectral density at frequency w
$\tau(w)$	Time delay at a frequency w of the cross spectral density
w	Angular frequency in radians per sec.

1. INTRODUCTION

Once food is ingested, it enters the stomach after passing through the esophagus. The stomach can be divided into three parts, the fundus, the corpus and the antrum as shown in Fig. 1.1. As the food enters the stomach, the fundus increases in size, like a balloon to receive the food. This process is termed receptive relaxation. The corpus and the antrum mix the ingested food with gastric juices and propel the material into the small bowel. This action is totally involuntary and during this stage there must be control of the direction of movement of food and its speed. The control system for these purposes would be complex considering the different requirements for different types of food, for example, liquids, solids, fatty acids, starch foods, sweet foods.

There are two separate control mechanisms that act in conjunction to regulate the movement of food in an orderly manner. They are: 1) Intrinsic Control mechanism (myogenic); 2) Extrinsic control mechanisms (neurogenic) [1]. These control mechanisms will be discussed with the stomach as an example. The Stomach is the best understood portion of the gastrointestinal tract.

1.1 Intrinsic Control Mechanisms

The intrinsic control of movement of food is exerted through the electrical activities generated in the muscular layers of the gastric

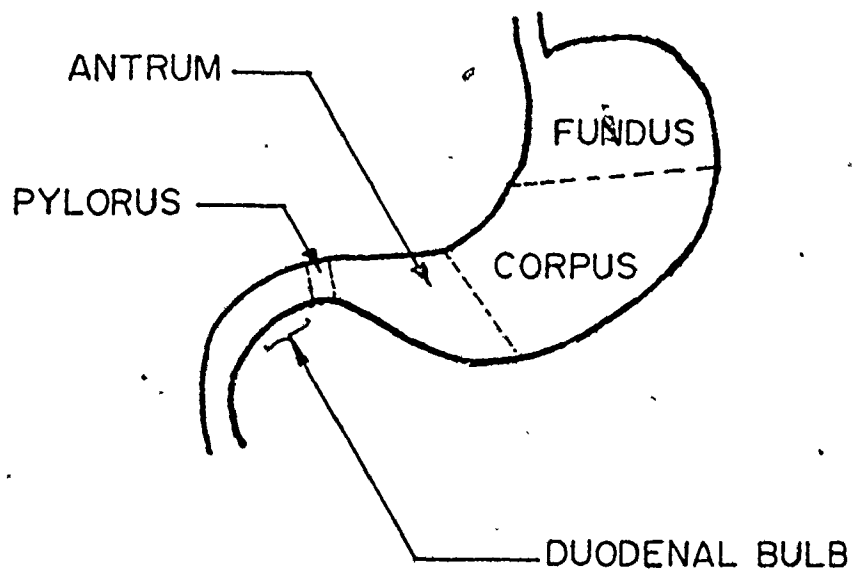


Fig. 1.1 Functional subdivisions of stomach

wall. Two types of electrical activities can be recorded from the smooth muscle layers of the stomach. The first type called Electrical Control Activity (ECA) [2] is omnipresent, rhythmic and has a frequency of about 3 control potentials/minute in man and about 5 control potentials/minute in dog.

The second type of electrical activity is called Electrical Response Activity (ERA) [2]. This consists of bursts of spikes (about 3 spikes/sec) and occurs in the phase immediately following a control potential. Each burst of spikes lasts for about 2 to 6 seconds in dog. This activity is associated with contractions i.e., whenever this activity occurs at any site in the gastric wall, a contraction is initiated at that site. Fig. 1.2 shows the gastric electrical activities recorded from an anesthetized dog.

The ECA does not cause contractions by itself. It controls the occurrence of the ERA and hence of contractions. The maximum frequency of contractions is thus limited by the frequency of the ECA. The control potentials do not occur simultaneously all over the electrically active region but show a definite phase lag pattern [3]. Longitudinal phase lag/cm is around 70 to 100°/cm near the most proximal site and around 8 to 20° near the pylorus. A control potential occurs first in the proximal stomach followed by a control potential at a distal site with some time lag and so on. Since ERA and a contraction is initiated soon after a control potential occurs, a ring of contraction seems to begin in the proximal stomach and moves distally, moving the gastric contents along with it. The contractions appear like a ring because there is very little phase lag among control potentials recorded by

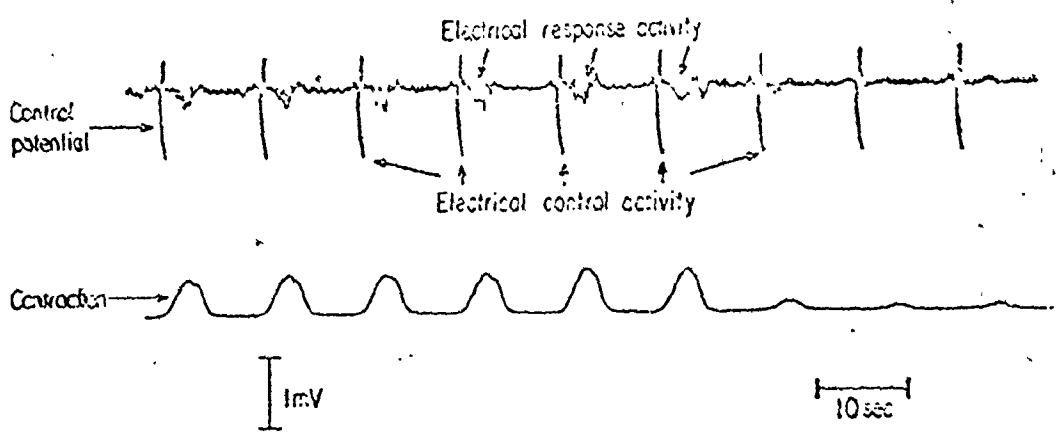


Fig 1.2 Electrical and mechanical activities recorded from an anesthetized dog.

electrodes implanted along the circumference of the stomach [1].

The gastric ECA is modelled as an array of bidirectionally coupled relaxation oscillators [3]. The intact and intrinsic frequency gradients and phase lag pattern observed in anesthetized dogs [3] could be simulated by such a model. A marked intrinsic frequency gradient was found along the axis of the stomach, and a slight intrinsic frequency gradient around the circumference from the greater curvature to the lesser curvature. Each oscillator in the array was represented by a system of two first order nonlinear differential equations [3].

1.2 Extrinsic Control Mechanisms

Extrinsic control mechanisms comprise the para-sympathetic, sympathetic and non-adrenergic nerves innervating the gastrointestinal tract. Vagus nerves innervating the gastric wall are the best understood at the present time. They cause contractions through the release of acetylcholine (Ach). It should be noted that occurrence of a control potential is a necessary but not a sufficient condition for the occurrence of a contraction. Ach must be present in sufficient quantities when a control potential occurs to result in a contraction.

1.3 Control Loop for Gastric Emptying [1]

The feedback loop showing the two control mechanisms which control the forward movement of food from the stomach into the small intestine is shown in Fig. 1.3 [1]. When the food is present in the stomach, it acts as a disturbance. Its presence is sensed by stretch and chemical receptors in the stomach and a signal is sent to the vagal center through efferent fibres. The vagal center sends signals through efferent fibres to release Ach from nerve endings. As discussed earlier,

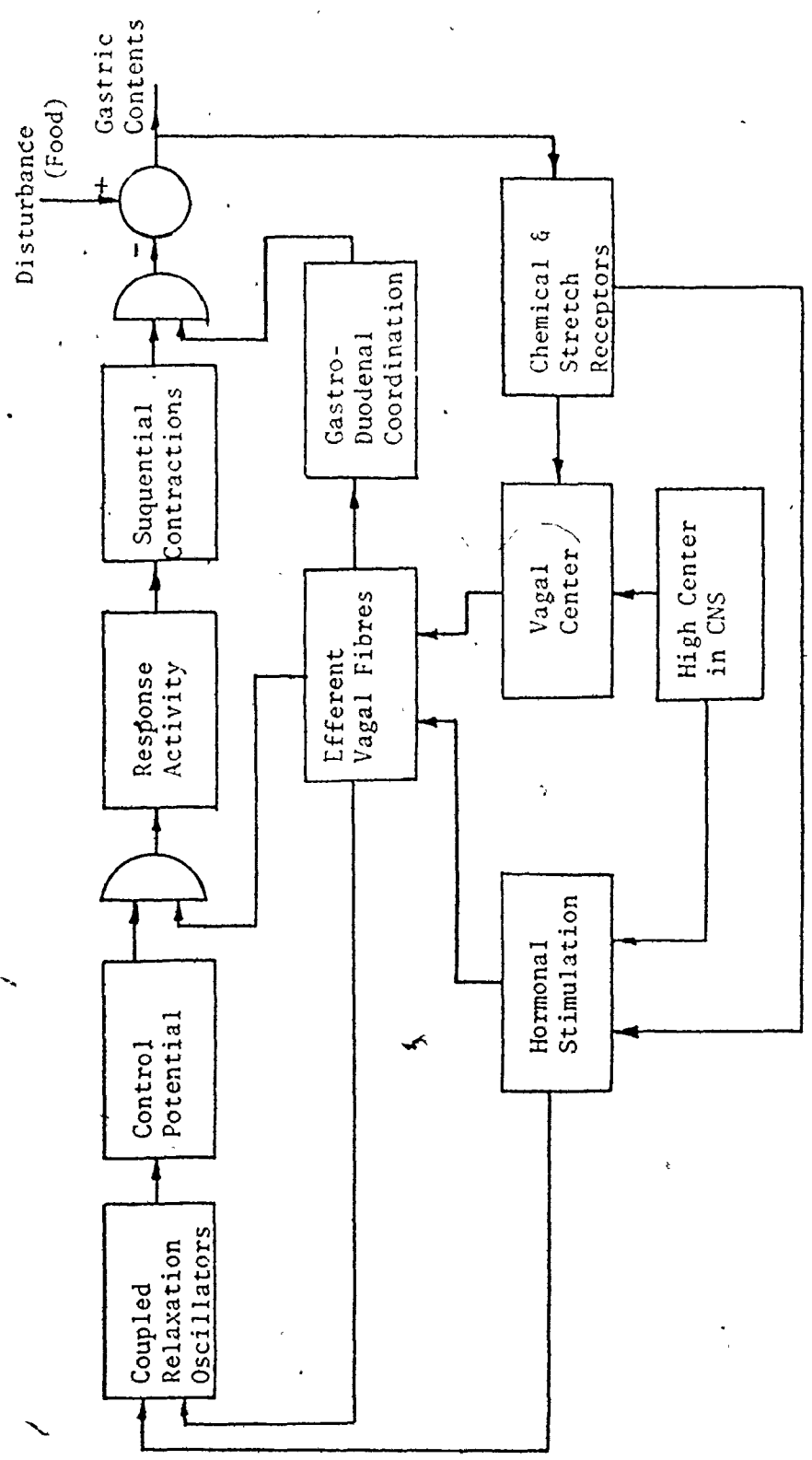


Fig. 1.3 A Feedback Control System for Gastric Emptying

both a control potential and release of Ach must occur at any particular site for a contraction and this is represented by an AND gate.

When a contraction reaches the pylorus, the gastric contents brought by the pyloric contraction should enter the proximal duodenum for emptying to take place. Once the food is in the small intestine its distal movement is controlled by a similar feedback control loop [4]. The frequency of ECA in the small intestine and the duodenum is in the range of 18.5 to 21 cycles/minute. This implies that the duodenum is capable of contracting at a higher frequency than that of the distal part of the stomach (Antrum). The antrum of the stomach and the duodenum could be considered as two control systems separated at the pylorus. The question that arises is whether they act independently or there exists a coordination between them. If they act independently, it is probable that a contraction in the duodenum has just begun and therefore it appears to be closed, when an antral contraction just approaches the end of the stomach to empty gastric contents. This would result in retropulsion and prevent the stomach from emptying. For the orderly movement of the food through the gastroduodenal junction, a coordination of the activities of the antrum, the pylorus and the duodenum is desirable. In other words, the proximal duodenum should contract following a pyloric contraction. This coordination and the contractions necessary for gastric emptying is represented by another AND gate. This coordination might be by electrical coupling across the pylorus, by a neural or hormonal pathway or could result from the mechanical, osmotic or chemical stimulus of the chyme propelled into the proximal duodenum.

The gastroduodenal interaction was investigated by Alvarez

and Mahoney [5] and others [5,6,7,8,9]. Alvarez and Mahoney were of the opinion that the pylorus acts as a block to the peristaltic waves from the stomach. Bass, Code and Lambert [6] reported that the ECA and the ERA detected in the antrum and the duodenum became attenuated and usually disappeared in the pylorus. They concluded that the pylorus acts as an electrical insulator.

E. Atanassova [7] studied the electrical activities of the stomach and the duodenum with intact gastroduodenal junction and with a section at the level of the pylorus. She reported coordination in the spike activities of the gastric and the duodenal walls - under conditions of hunger and peristalsis after feeding and upon mechanical stimulation. Following a section at the level of the pylorus, dissociation between the spike activities of the gastric and the duodenal walls was observed. Periods of spike activity of gastric wall without any corresponding activity of the duodenal wall and conversely periods of spike activity of the duodenal wall alone accompanied by a relative inhibition of the gastric wall were observed. Similar conclusions about the coordination were drawn by Allen, Poole and Code [8], and McCoy and Bass [9]. A gastric peristaltic wave moves down the antrum and ends in a pyloric and duodenal contraction. This implies that the antrum, the pylorus and the proximal duodenum function as a coordinated unit that is timed both to promote gastric emptying and to prevent reflux from the duodenal cap to the stomach. Papazova, Atanassova and Rodoeva [7] also reported coordination in the contractile activities of the stomach and the duodenum.

Bortoff and Davis [10] studied the gastroduodenal junction

with the aim of finding the mechanism for the coordination. They observed the transmission of the antral control waves across the junction. The antral control waves were shown to spread through the junction to the proximal duodenum where they periodically augmented depolarizations associated with the duodenal control waves, thereby increasing the probability of duodenal spiking. The duodenal spread of the antral control waves was concluded to be a myogenic process. The duodenal electrical recordings were made within 17mm from the junction.

There is no mention of coordination or interaction across the gastroduodenal junction when the stomach is empty. All of the previous conclusions were based on visual analysis which are subjective. The present study is undertaken to study the coordination by analysing the signals using a computer. The information regarding the gastroduodenal coordination (periodic augmentation of one wave by another) could be extracted by spectral analysis of the electrical and mechanical signals. The computed spectrum of a signal gives the frequency components of which the signal is composed. From this information, it is possible to detect the frequency components corresponding to the antral and the duodenal electrical and mechanical activities, even when the signals concerned are noisy and complex.

The studies were done in dogs. The methods employed, experiments conducted for this purpose and the computer techniques employed are discussed in chapter 2. The computer programs developed for this purpose are also described, with appropriate flow-charts, in the chapter 2. The source code listings of the programs and the subroutines developed are given in Report GIR-1, Bio-Medical Group, Department of

Electrical Engineering, McMaster University, Canada.

The results of the study are given in chapter 3. The conclusions and suggestions for future work are discussed in chapter 4.

2. METHODS

2.1 Methods

Six healthy dogs were used to study the coordination of the antral and duodenal activities. Three electrodes for monitoring the electrical activity and three strain gauges for monitoring the mechanical activity were surgically implanted by using pentobarbital anesthesia (27 mg/kg). One strain gauge and electrode were at the pylorus. The distances of the antral and the duodenal electrodes and strain gauges from the pylorus in each dog are shown in the following table.

Dog No.	Antral Electrode	Antral Strain gauge	Duodenal Electrode	Duodenal strain gauge
1	3.4 cm	3.8 cm	3.8 cm	2.8 cm
2	1.2 cm	2.5 cm	1.9 cm	2.5 cm
3	3.5 cm	2.7 cm	4.0 cm	3.2 cm
4	3.0 cm	4.1 cm	2.0 cm	3.6 cm
5	4.0 cm	3.5 cm	1.5 cm	2.5 cm
6	2.5 cm	3.0 cm	5.0 cm	4.0 cm

The dogs were allowed to recover for one week before any experiments were conducted. The position of strain gauges and electrodes are shown in Fig. 2.1.

2.2 Measurement of Electrical Activity

Bipolar electrodes of platinum iridium wire of 0.15 cm diameter

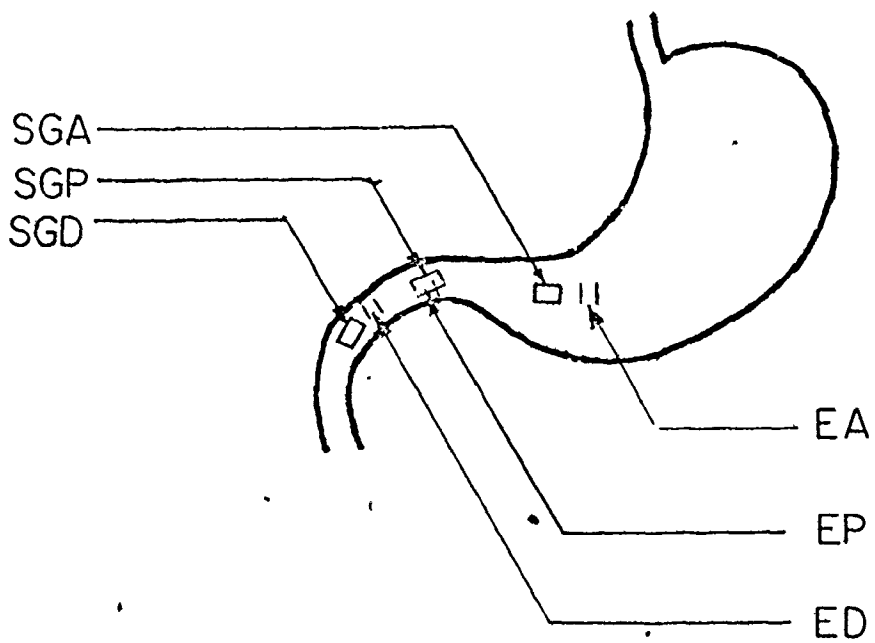


Fig.2.1: Position of implanted electrodes and strain gauges.

and 1 cm long were used. The recordings were made on an eight channel recorder with lower and upper cut off frequencies of 1.6 and 22 Hz respectively. [Type R, 8 channel, rectilinear recorder, Beckman Instruments.] The recordings were made simultaneously on a Philips 7 channel tape recorder. The signals were later fed into a Nova 830 mini-computer for subsequent analysis.

2.3 Measurement of Mechanical Activity

Strain gauges are preferred over other methods such as balloons for monitoring mechanical activity because of the following advantages.

- a) They record the contractile activity of the muscle directly.
- b) They are sewn on the outer surface of the organ. Thus their use avoids any interference with the flow of intra-luminal contents and avoids stimulation of internal receptors. Since they are permanently fixed in position, the same site can be monitored repeatedly without using elaborate methods to place the sensors in the desired position.

Strain gauges were assembled in the laboratory. The methods employed were similar to those reported by Bass and Wiley [11]. Strips of Berylco 25 Alloy (Beryllium corporation, Reading, Pa.) were cut into pieces of 3.5 x 12 mm in size and shaped to an arc of 7/16 inch radius of curvature. The strips were tempered by placing them in an oven at 600° F for one hour and dropping them quickly into cold water after removal from oven. The surfaces were sanded with 180 grit silicon carbide (Manufactured by Micro Measurements, Inc., Romulus, Michigan), rinsed with isopropyl alcohol and stored in a clean place. Strain gauge elements used were EA-06-036TS-120 series, 120 ohms \pm 2% resistance of Micro Measurements. The back of the gauge element was cleaned with

neutralizer, rinsed with isopropanol and air dried. The strain gauge element was bonded to Cu-Be Strip with a thin layer of M Bond 610 (Manufactured by Micro Measurements). The gauges were again cleaned with petroleum ether followed by isopropanol. The three solder tabs of the gauge were tinned with cored tin-lead solder and lead wires, consisting of three Teflon insulated 32 AWG wires enclosed in a silicone jacket, were attached. The units were coated with E712 epoxy resin for water proofing and cured to hardness at room temperature.

The leads from the electrodes and strain gauges were brought out through the abdominal wall and terminated at a female Amphenol Connector embedded in a stainless steel cannula sutured to the abdomen.

2.4 Experiments

The dogs were trained to stand still with harness attached. A connection to the recording instrument was made by means of a cable. They were fasted for 24 hours prior to each experiment. The recordings were made for about 30 minutes before feeding and for about one hour after feeding.

Six experiments on each dog were conducted after a standard meal (1 can of dog food). Six other experiments on each dog were conducted with pentagastrin administered intravenously at 4 mgm/kg/hr. Pentagastrin releases hormones that initiate peristaltic contractions in the stomach. Presence of food in the stomach also releases gastrin.

In a few experiments, Atropine 45 µg/kg was given intravenously after food or pentagastrin to study the interaction of the electric activity of the gastroduodenal junction when mechanical activity was inhibited. [Atropine releases hormones that inhibit mechanical contrac-

tions.]

2.5 Computer Analysis of Signals

The antral, the pyloric and the duodenal electrical and mechanical activity signals were analysed on a Nova 830 Mini-Computer to study their interaction. The facilities available in the Mini-Computer are shown in Fig. 2.2.

The major steps in the analysis are:

- a) Data acquisition - to accept the analog signals from the tape recorder, convert them into discrete digital data and store the data in disc files for subsequent use.
- b) Display of a selected segment of data on the graphic terminal of the computer for visual examination.
- c) Extraction of suitable parameters of the signals descriptive of the activities of the muscles.

The schematic diagram of the analysis program is given in Fig. 2.3.

The signals recorded in the region of gastro-duodenal junction show considerable variation in waveshape and amplitude. But, as discussed in Chapter 1, the antral and the duodenal ECA are characterized by two distinct frequencies of about 4 cycles/min and 18 cycles/min respectively. The mechanical activity at a particular site is determined by the maximum rate of ECA frequency. A coordination between two activities, say between the electrical activities of the antrum and the duodenum, may result in a periodic augmentation of the duodenal electrical activity at the antral frequency. In view of this, the frequency is of prime importance in analysing these signals. The frequency of ECA and mechanical contractions remains stable in a dog in the fasted state, fed state.

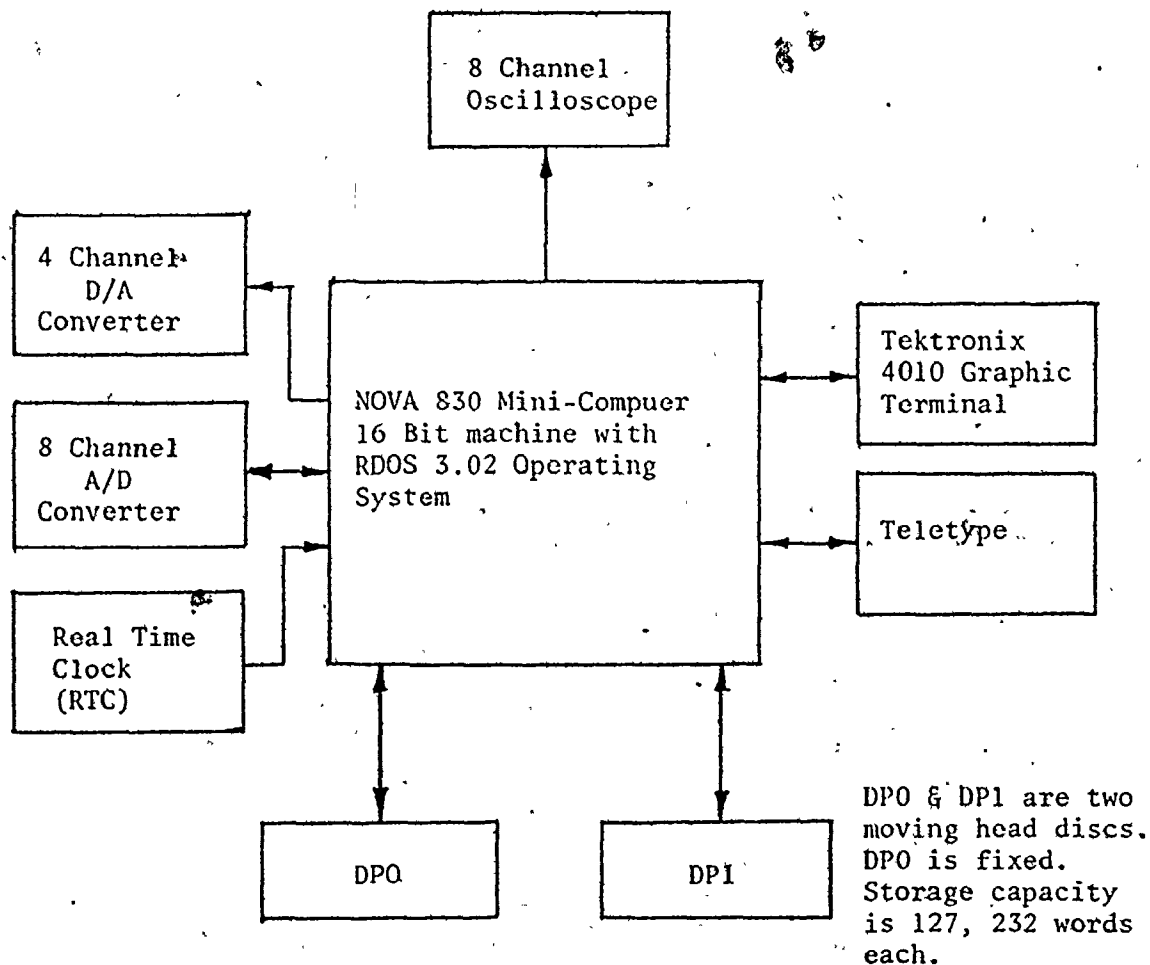


Fig. 2.2 Digital Signal Processing Facilities

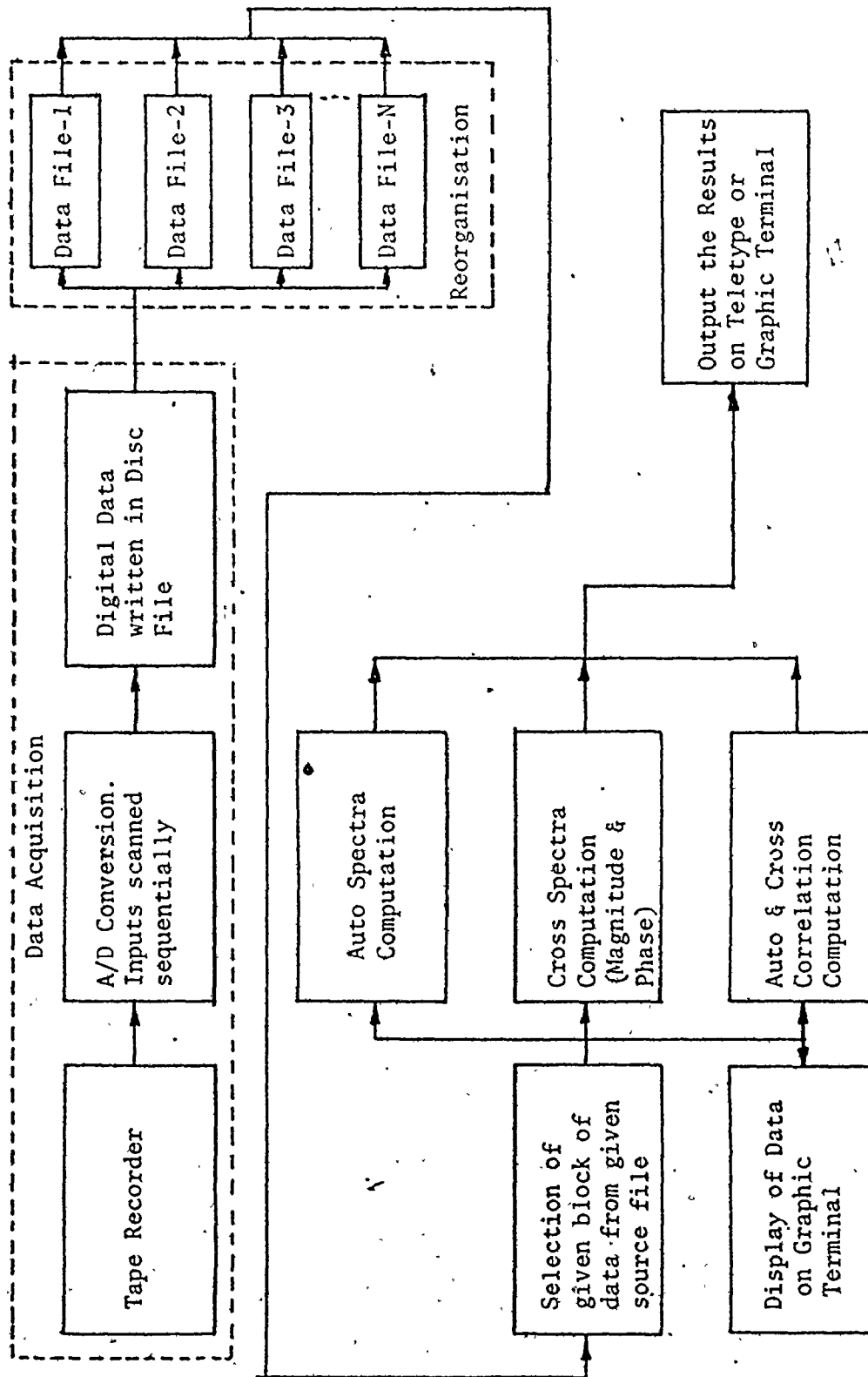


Fig. 2.3 Schematic diagram of Analysis Programs

and when the drugs were given. [The frequency may be different in each state, e.g. the ECA frequency increases when pentagastrin was given. It remains stable at the increased value.] This information can be obtained by computing the following:

- a) Auto power spectral density
- b) Cross power spectral density - both amplitude and phase information.

These are defined later.

2.5.1 Data Acquisition

The antral, the pyloric and the duodenal mechanical and electrical signals are recorded on an analog tape recorder. The analog signals must be converted into discrete digital data for computer analysis. This necessitates the following:

- a) sampling of the analog data at an appropriate frequency.

Preliminary spectral analysis of signals (methods explained in later sections) indicated negligible energy at frequencies above 1 cycle/sec. Hence a sampling frequency of 10 cycles/sec which is higher than the nyquist rate [12] is employed in the present work.

- b) Analog to Digital conversion - the eight channel A/D converter available on the computer is used for this purpose. The specifications of the A/D converter are [13]:

Input voltage:	±5 Volts
Output Code:	12 bits, 2's complement form (signed)
Resolution:	2.4 m volts
No. of input channels:	8

Errors that may be introduced into computed spectral density

due to quantization and aperture time (finite time of A/D conversion) can be considered insignificant, as the range of signals (both electrical and mechanical) encountered in the present study is much higher than the resolution of the A/D converter and conversion time is small compared with sampling period.

The flow-chart of the program "ACQ" developed for the above purpose is given in Fig. 2.4. The A/D converter and Real Time clock (RTC) of the computer are program controlled. The program comprises two tasks. The first, as shown in the flow chart, creates the second task and enters into delay mode. The Delay period can be controlled in integral multiples of system RTC period.

The second task is activated, once the first task enters the delay mode. It initiates the A/D conversion from channel 0 and scans the programmed number of channels. The converted digital data is subsequently written into disc file for later use. This part of the program is written as a subroutine entitled "ADCON". Due to limitation in the execution time, it was not possible to write the data from each channel in separate files within one sampling period. The data are interlaced. The reordering of the data from each channel into distinct files is carried out by another program entitled "ORDER". The source code listings of the programs "ACQ" and "ORDER" are given in reference 14.

2.5.2. Display of Data.

Gastroduodenal interaction is studied by analysing signals of 102.4 seconds duration before and 15, 30 and 45 minutes after food or pentagastrin infusion. The location or address of the desired segment within a file can be identified by viewing the data plotted on the

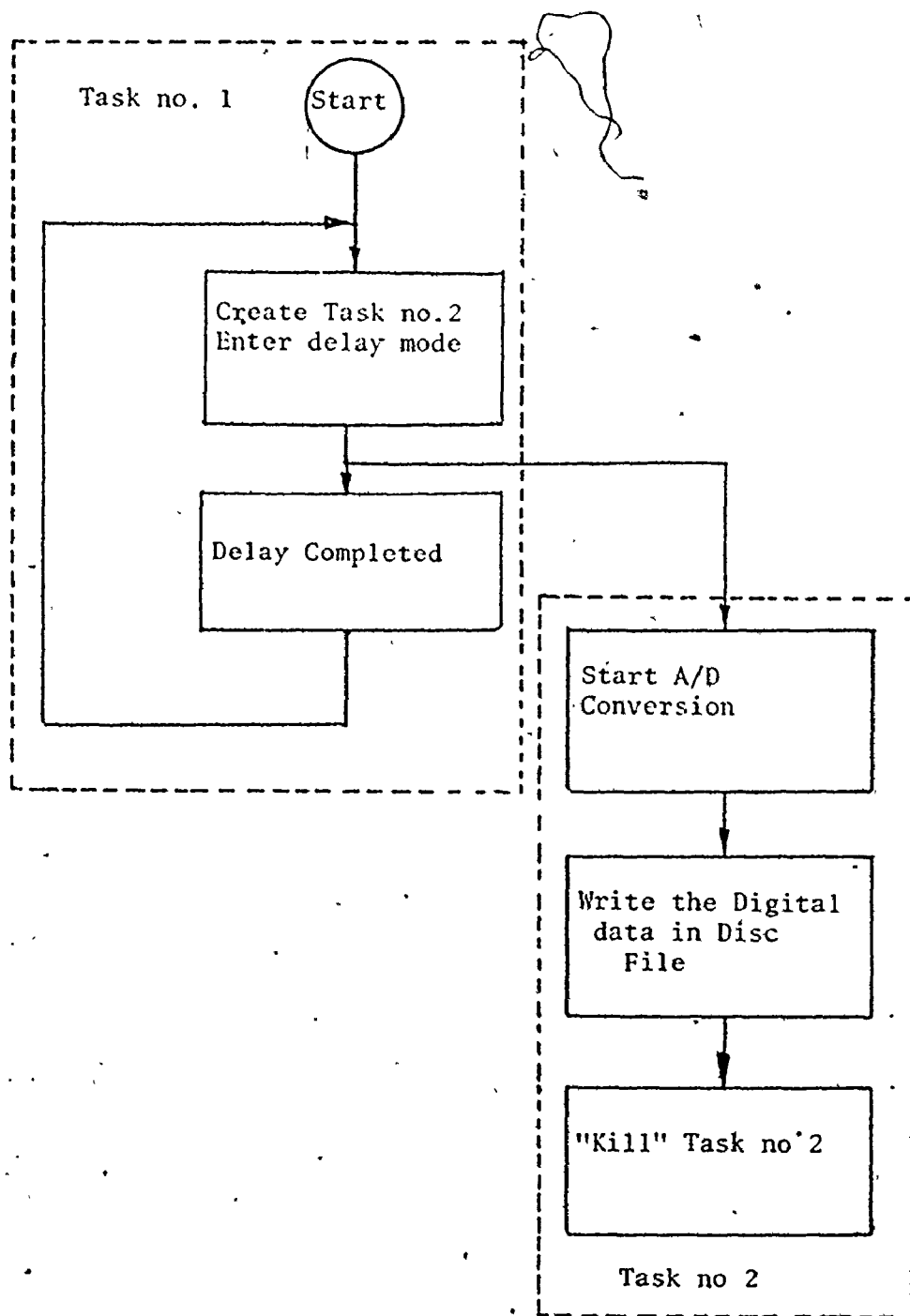


Fig. 2.4 Flow-Chart for Data Acquisition Program

graphic terminal. The programs written for this purpose are interactive. The flow chart of the program is shown in Fig. 2.5. It achieves the following:

- a) Accepts the file name and block no. of a segment to be displayed through the Tektronix Graphic Terminal 4010 attached to the computer.
- b) Reads the selected block of data from the disc file and writes into the computer main memory as a one dimensional array.
- c) This array is scaled appropriately so that the range of the data (the difference between the maxima and minima) is accommodated within the display capacity of the Graphic terminal (780 for 4010 terminals).

If the range is greater than 780, the data is divided by a factor

$$M = \text{Integral part } \left[\frac{\text{Range}}{780} \right] + 1 .$$

If it is less than 780, the data is multiplied by a factor

$$M = \text{Integer } \left[\frac{780}{\text{Range}} \right]$$

- d) Plots the data with magnitude on the Y-axis. The x-axis represents the time/position of the data in the array. A maximum of 1023 discrete points may be displayed [15]. The adjacent points are joined by a straight line.

The listing of the program titled "ANAL" and other subroutines used in the program are given in reference 14.

2.5.3 Computation of Auto Power Spectral Density (PSD)

The computation of power spectra could be done by three different methods [17].

- a) The standard or Blackman-Tukey Method. This method utilizes the Weiner-Khinchin relation to obtain the spectrum from the Fourier

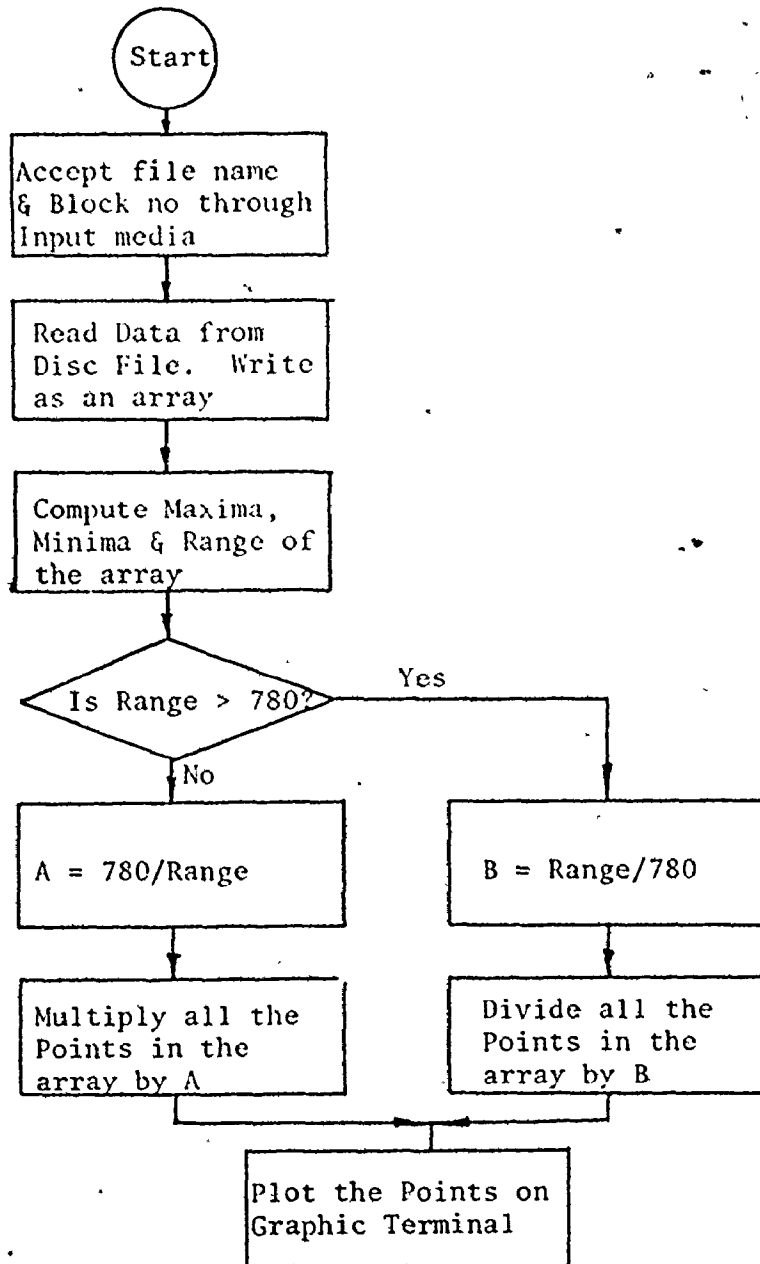


Fig. 2.5 Flow-Chart for the Display of array of Points on the Graphic Terminal

Transform of correlation function [16].

b) Filtering approach. In this method, PSD is obtained at a specific frequency by passing the data through a bandpass filter, squaring and averaging the output.

c) The Direct Fourier Method. This method using Fast Fourier Transform algorithms is faster than the other two methods and hence it was adopted in the present work.

Computational Procedure for PSD

The PSD $S_N(\omega)$ of an observed data sequence of length N is related to the Discrete Fourier transform of the sequence as follows [17]:

$$S_N(\omega) = \frac{1}{N} \left| \sum_{n=0}^{N-1} x_n e^{-j\omega T_s n} \right|^2 \quad (1)$$

$$= \frac{1}{N} \left| X_N(\omega) \right|^2 \quad (2)$$

Equation (2) suggests the following computational procedure.

- a) Read the data from the source file.
- b) Compute the mean of the data sequence and remove the dc component if required.
- c) Compute the Discrete Fourier Transform of the data sequence using FFT algorithms.
- d) Compute the power spectral density by squaring the magnitude of the DFT coefficients computed in step (c).

When analysing a record of longer duration (say 6000 data-points), two methods can be used. The first approach is to compute the DFT of the complete data. The second is to divide the data into

equal subsequences of smaller length (1024 points in our case). The subsequence $x_r(n)$ is related to the original sequence as

$$x_r(n) = x[n + (r-1)D], \quad r = 1, 2, \dots, k \quad (3)$$

where $D = 1024$.

The PSD of each subsequences are computed serially in time. Then the PSD of the entire sequence is computed as

$$S_N(w) = \frac{1}{K} \sum_{r=1}^K [X_r(w)]^2 \quad (4)$$

If each subsequence is considered as an ensemble of a stochastic process, the variance of the spectral density is reduced by a factor of $1/K$ of individual variance [18].

The second approach is used in the present work for the following reasons.

a) Due to the limitation on available memory size in the computer, the complete data in a disc file cannot be written in the active memory. Data has to be accessed from the disc when required during computation in the first approach. As this necessitates the opening and closing of files, byte pointer generation and its setting, the computation time will increase. In the second approach, due to the smaller length of a subsequence, it is feasible to transfer the data from the disc into active memory for one subsequence at a time.

b) If the sampling frequency is constant, the frequency resolution of the computed results keeps changing as the length changes in the first approach.

The number of points used in the computation of the DFT of a segment of data is 1024. This gives a frequency resolution [19]

$$\Delta f = \frac{f_s}{1024} = 0.585 \text{ cycles per minute for } f_s = 10 \text{ Hertz.}$$

This resolution is adequate for the present application.

As explained before, there is a considerable variation in waveshape and amplitude of signals and hence a large variation in the magnitude of PSD at a particular frequency from record to record is expected. Since the frequency is of prime importance rather than the magnitude of PSD in the present study, no attempt is made to reduce the errors in the computation of PSD due to leakage on account of the finite no. of data points with windowing techniques [17].

The flow-chart of the program for the above purpose is given in Fig. 2.6. The file name and Block number of the data to be analysed are fed by the operator through the graphic terminal. Each block consists of 1024 points. The source data stored in the disc files in real integer form is converted into floating point complex number form with zero imaginary part for subsequent computation. The converted 1024 data points are written as one dimensional complex array in the active memory. This part of the program is written as a subroutine "DACON". The DFT of the complex array is computed by another subroutine "FFT". The DFT coefficients computed are not in the natural order, i.e. its coefficients are not arranged in the order of increasing frequency. The rearrangement of the coefficients in natural order is accomplished by the subroutine "BITR" using the commonly used bit reversal algorithms [20]. The Square of the magnitude of each DFT points is computed by the subroutine "SPDN".

When computing the PSD of long records as discussed before, the intermediate results after the computation of each section have to

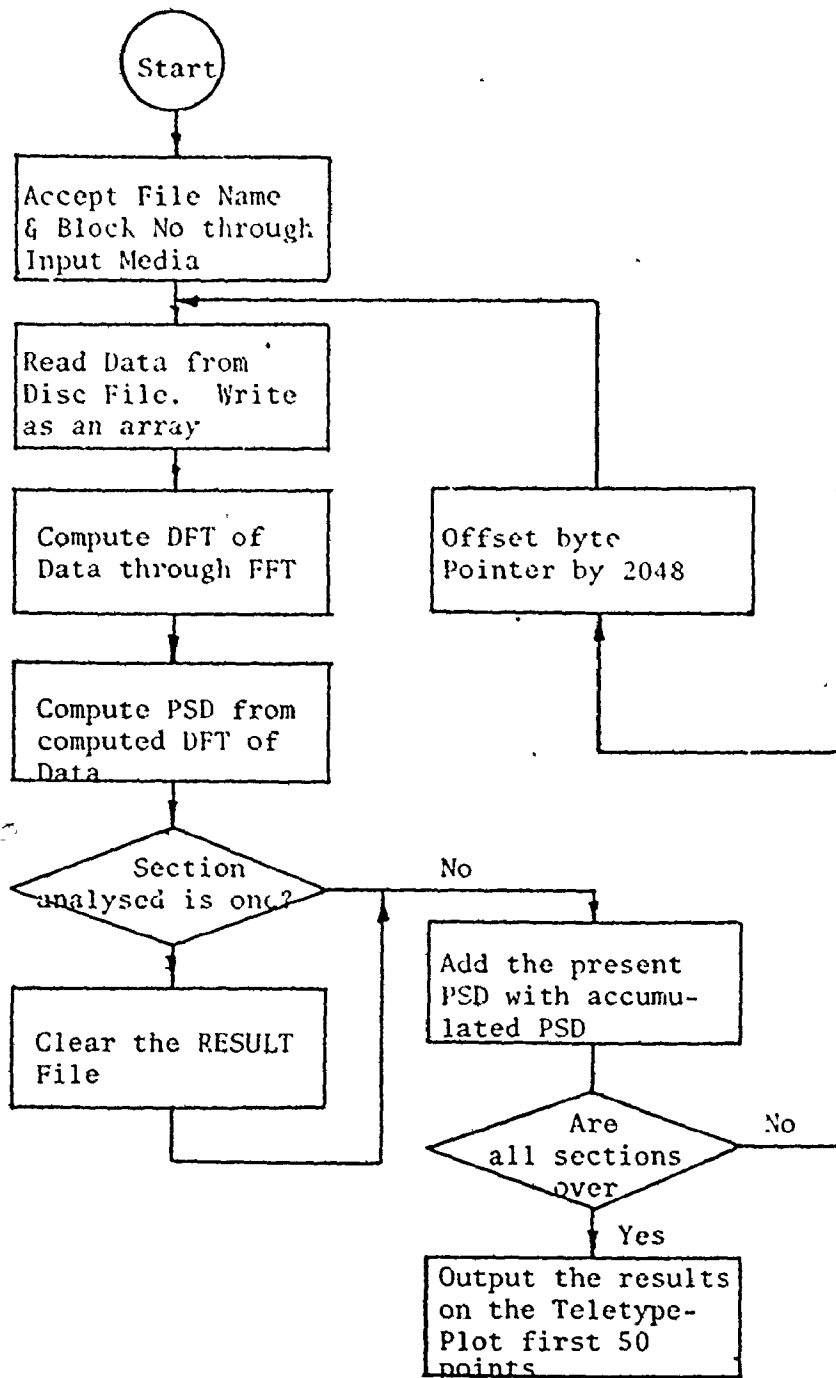


Fig. 2.6 Flow-Chart for Computation of Auto Power Spectral Density

be saved for subsequent use. Due to memory size limitations, intermediate results are stored in a disc file named "RESLT". The PSD for the first 50 discrete frequency points covering a frequency range from 0 to 29.25 cycles/minute are outputted. The results are also plotted on the teletype.

The listings of the program entitled "POWLR" and the sub-routines used are given in reference 14.

2.5.4 Computation of Cross Spectral Density

The cross spectral density of two signals enables one to find the common frequency components on the signals. The presence or absence of the augmentation of the duodenal signals at the antral frequency in the present study could be determined by computing the cross spectral density between the two signals.

The expression for the cross spectral density of two data sequences $x(n)$ and $y(n)$ is [17]

$$S_{xy}(w) = \frac{1}{N} X_N^*(w) Y_N(w) \quad (6)$$

It involves the Fourier Transform of $X_N(w)$ and $Y_N(w)$. The cross spectrum is complex valued. Magnitude and phase angle are given by

$$|S_{xy}(w)| = \frac{1}{N} |X_N(w)| |Y_N(w)| \quad (7)$$

$$\phi_{xy}(w) = \angle Y_N(w) - \angle X_N(w) \quad (8)$$

The time delay of a particular frequency component in the two signals is obtained from the phase angle of the cross spectrum by the following expression [21]

$$\tau(w) = \frac{\phi_{xy}(w)}{2\pi f} \quad (9)$$

Equations (4-7) suggests the following computational procedure for the computation of cross spectral density.

- a) Read the given data from the source files.
- b) Compute the mean of each data sequence and subtract the mean from the original data.
- c) Compute the discrete Fourier Transform of the two data sequences $x(n)$ and $y(n)$.
- d) Compute the magnitude of DFT coefficients of the two data sequences $|X_N(w)|$ and $|Y_N(w)|$.
- e) The cross power spectral density magnitude $S_{xy}(w)$ is computed by multiplying $|X_N(w)|$ and $|Y_N(w)|$.

The flow-chart of the program for this purpose is shown in Fig. 2.7.

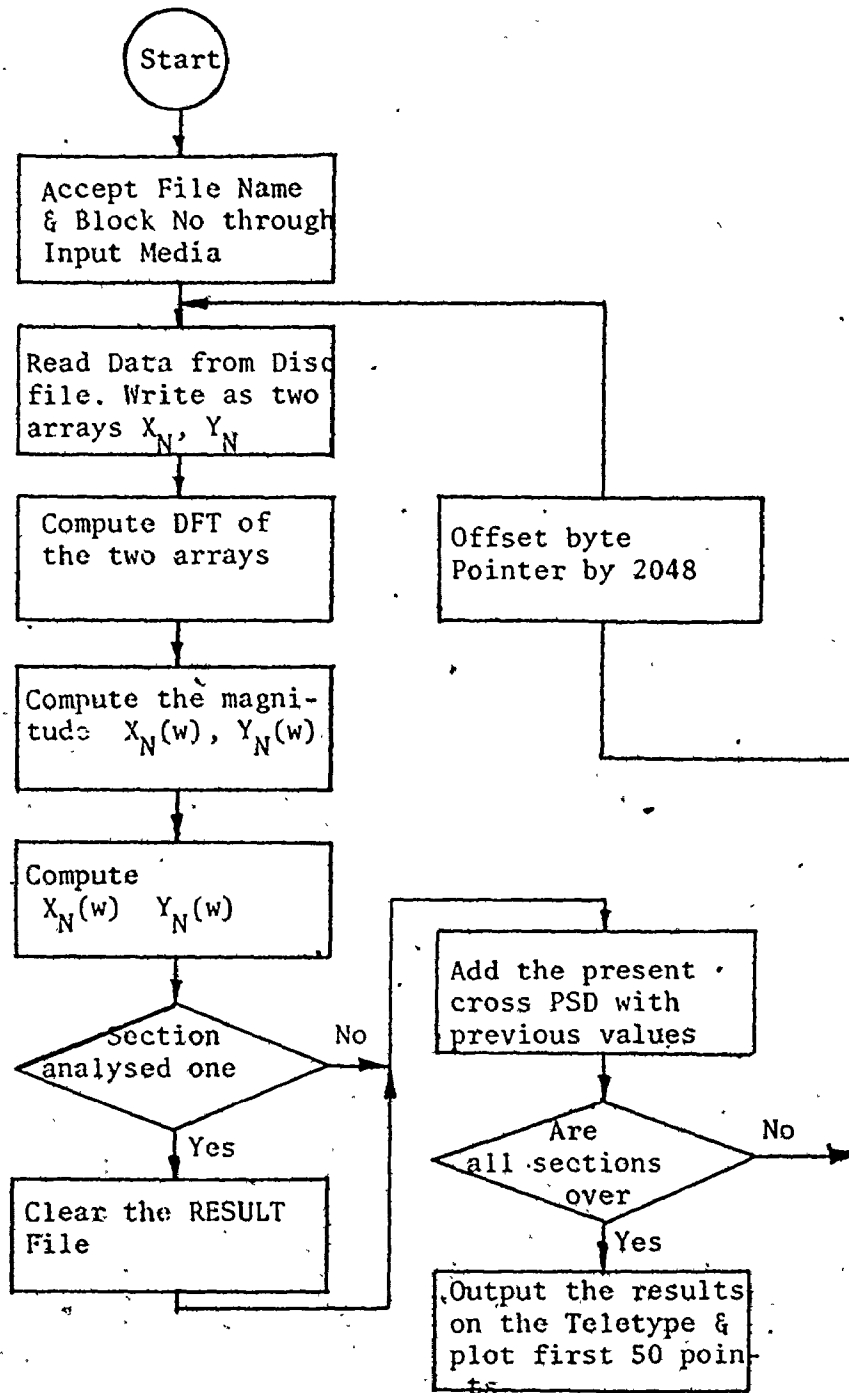
To find the phase angle of the cross power spectral density, steps d and e above are substituted by the following

- f) Compute complex conjugate $X_N^*(w)$ of the data sequence $x(n)$.
- g) Compute $S_{xy}(w)$ by multiplying $X_N^*(w)$ and $Y_N(w)$.
- h) Compute the phase angle

$$\phi_{xy}(w) = \tan^{-1} \frac{\text{Imaginary part of } S_{xy}(w)}{\text{Real part of } S_{xy}(w)}$$

- i) Compute the time delay $\tau = \frac{\phi_{xy}(w)}{2\pi f}$.

The listing of the program "CRSPM", "CRRL" and the subroutines employed for this purpose are given in reference 14.



3. RESULTS

As discussed in chapters 1 and 2, the interaction between the pyloric and duodenal electrical and mechanical activities was studied by computing the auto and cross power spectral density of signals. The signals were recorded in the fasted state, and 15, 30 and 45 minutes after a meal and after intravenous infusion of pentagastrin at 4 $\mu\text{g}/\text{kg}/\text{hr}$.

The electrical and mechanical signals recorded from the pylorus and the duodenum in the fasted state in one dog (Dog #5) along with their computed auto spectra is shown in Figs. 3.1 - 3.3. The magnitude of PSD is plotted against discrete frequency, with the maximum value normalised to unity. The discrete frequency points are at intervals of .585 cycles per minute. Figs. 3.2 and 3.3 show that both the pyloric and the duodenal electrical activities have a component at antral frequency of 5.26 cPM. The duodenal electrical activity also shows a component at a frequency of 17.5 cPM (duodenal control frequency). Other components seen in the PSD are random in nature and are accounted for by the random variation in waveshape. The mechanical signals are not analysed in the fasted state, as in most cases there is very little activity.

The signals recorded 10 minutes after food and their spectra are shown in Figs. 3.4 to 3.8 for the same dog. As in the previous case,

a component at antral frequency is seen in both the pyloric and the duodenal electrical and mechanical activities. The marked difference from the previous record is that the magnitude of spectral density at the antral frequency increased in the duodenal recording.

The electrical and mechanical signals recorded in dog no. 5 4 minutes after pentagastrin and the computed spectra are shown in Figs. 3.9-3.13. The Antral frequency component at 5.8 c/min is seen both in the electrical and mechanical activity of the duodenum. The signals recorded after atropine and the computed spectra of the electrical activity of the duodenum are shown in Figs. 3.14-3.15. Both the antral frequency and the duodenal frequency components are seen.

Considering the results for all five dogs, the presence or absence of a component at the antral frequency in the duodenal electrical and mechanical activities derived from the autospectra as explained above is indicated in Tables 3.1 - 3.8. Relative changes in the magnitude of PSD at the antral frequency in the duodenal electrical activity are indicated.

Column headings A, B, C, D and E denote the following:

- A: Antral frequency component in the pyloric electrical activity
- B: Antral frequency component in the duodenal electrical activity
- C: Antral frequency component in the pyloric mechanical activity
- D: Antral frequency component in the duodenal mechanical activity
- E: Duodenal frequency component in the pyloric electrical activity.

Entry X in a column indicates presence, blank indicates absence and a dash indicates data not available. The data is not available in certain cases due to defective strain gauges or their premature failure.

The magnitude of the computed cross power spectral density of two signals indicates their common frequency components. As this information is also available from the auto power spectral density of the individual signals, information extracted from the magnitude of the cross power spectral density computations is redundant. Phase lag information at different frequencies was obtained from the phase of the cross spectra computations; because of differences in the waveforms of the signals which were cross-correlated, the phase information does not yield measures of physical delay. Consequently all cross-correlation calculations were not used in arriving at the conclusions.

GASTRODUODENAL ELECTRICAL &
MECHANICAL ACTIVITIES (fasted)

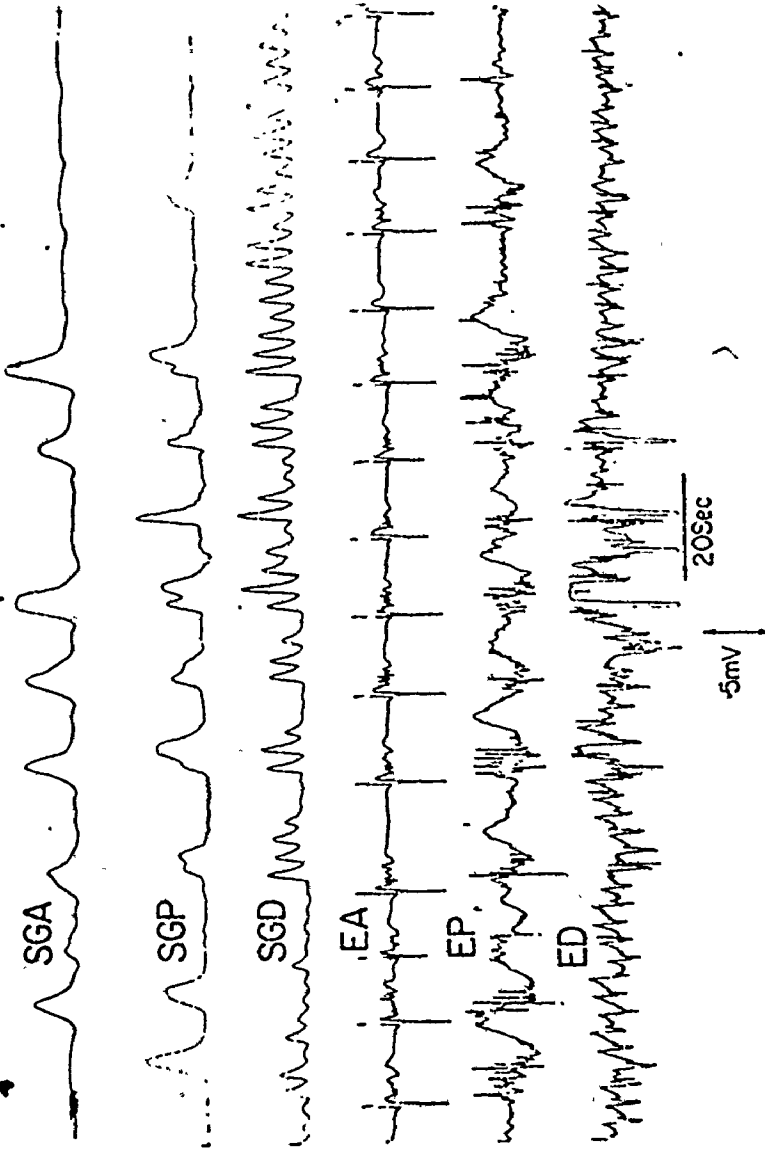


Fig 3.1: Electrical and Mechanical activities recorded
from a dog. (Fasted state)

POWER SPECTRUM- PYLORIC ELECTRICAL
ACTIVITY (fasted)

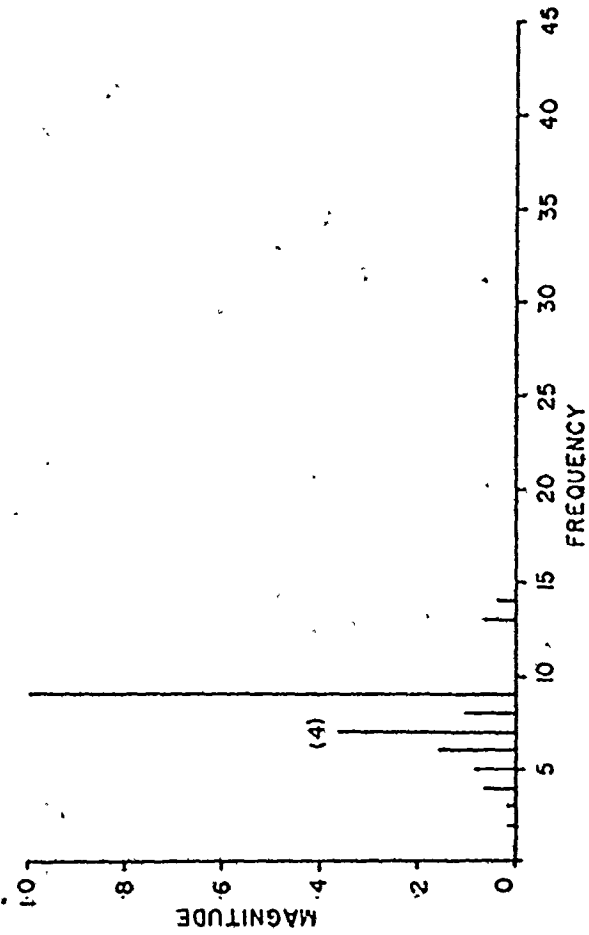


Fig 3.2: Power Spectral Density of the Pyloric Electrical activity (Fasted state)

POWER SPECTRUM - DUODENAL ELECTRICAL ACTIVITY (fasted)

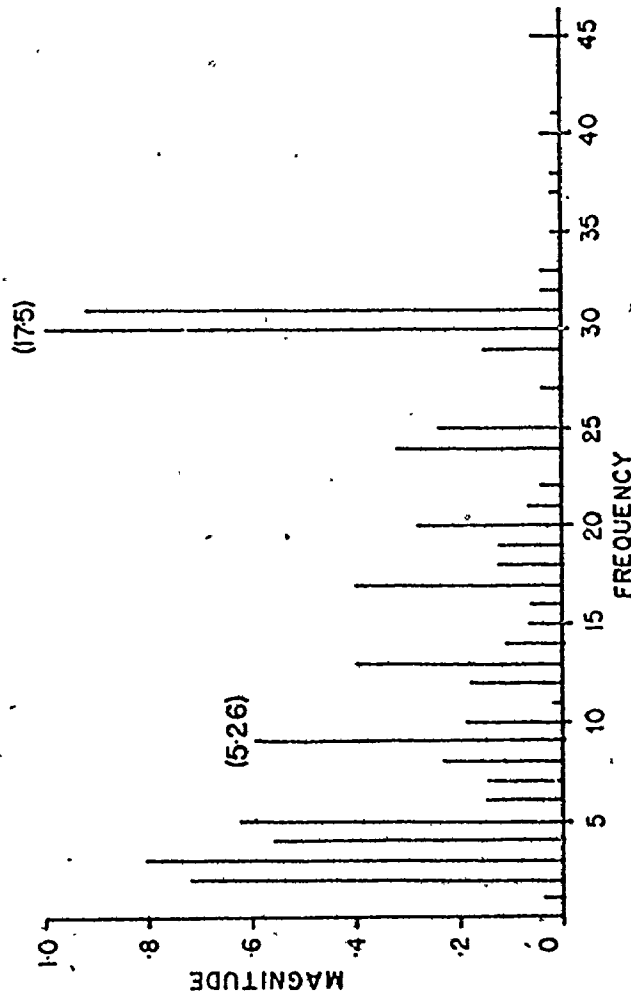


Fig 3.3: Power Spectral Density of the Duodenal Electrical activity. (Fasted state)

GASTRODUODENAL ELECTRICAL &
MECHANICAL ACTIVITIES (10 min)

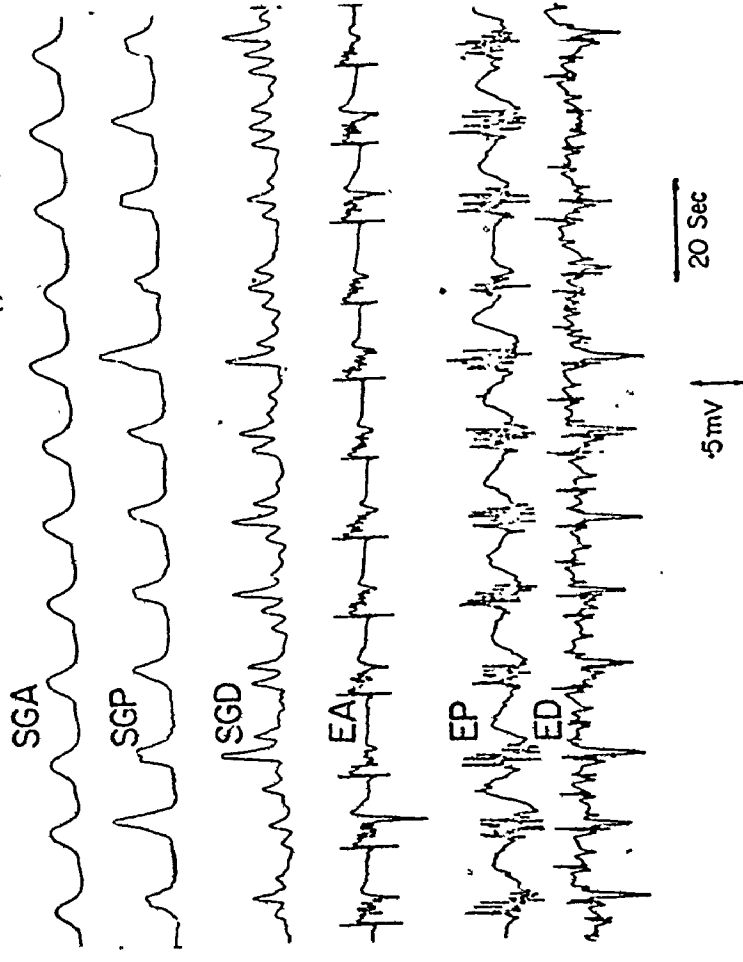


Fig 3.4: Electrical and Mechanical activities recorded from a dog. (10 Minutes after feeding)

POWER SPECTRUM- PYLORIC ELECTRICAL
ACTIVITY(10min)

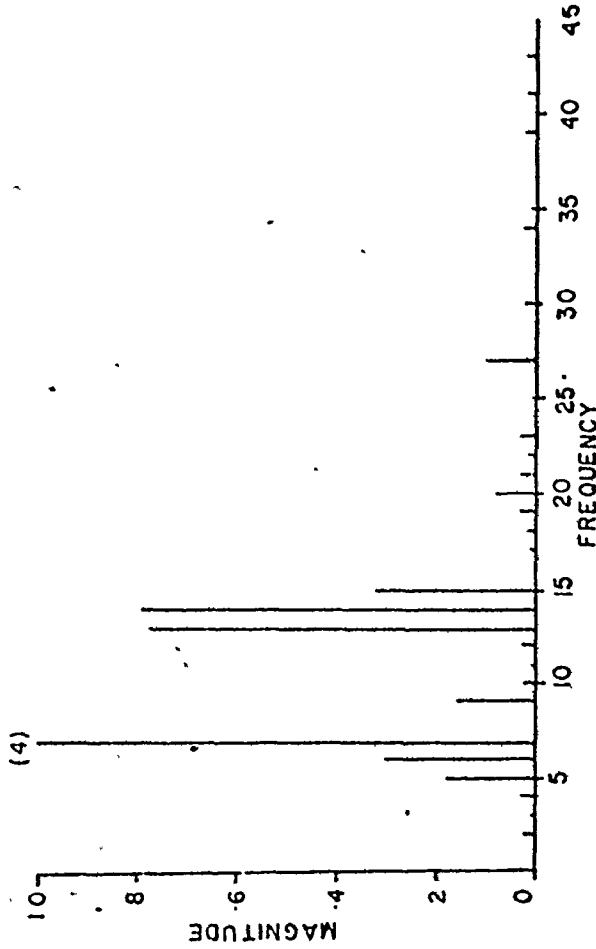


Fig 3.5: Power Spectral Density of the Pyloric Electrical activity- 10 minutes after feeding.

POWER SPECTRUM-DUODENAL ELECTRICAL
ACTIVITY(10min)

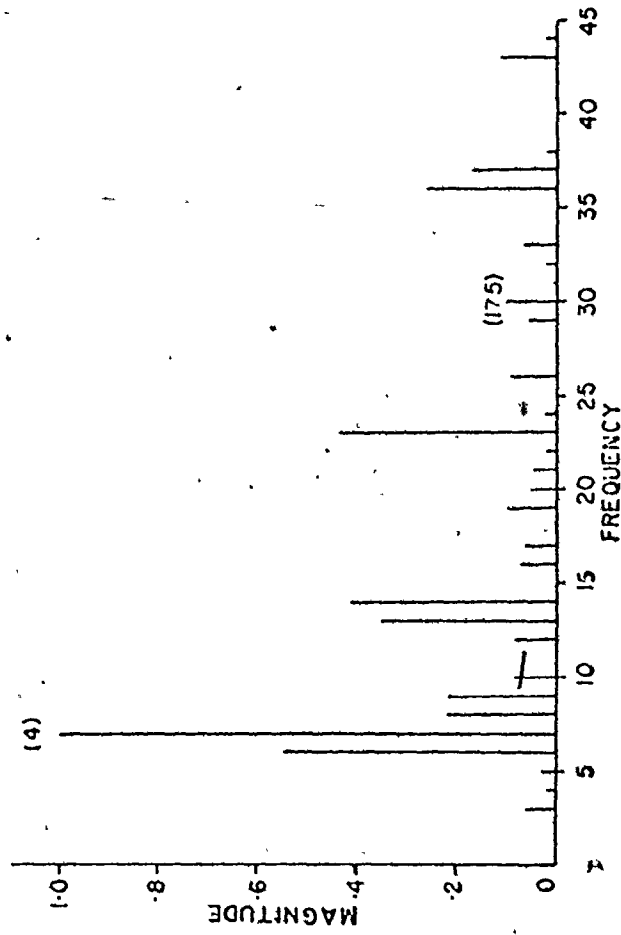


Fig 3.6; Power Spectral Density of the Duodenal Electrical activity- 10 minutes after feeding.

POWER SPECTRUM- PYLORIC MECHANICAL
ACTIVITY(10min)

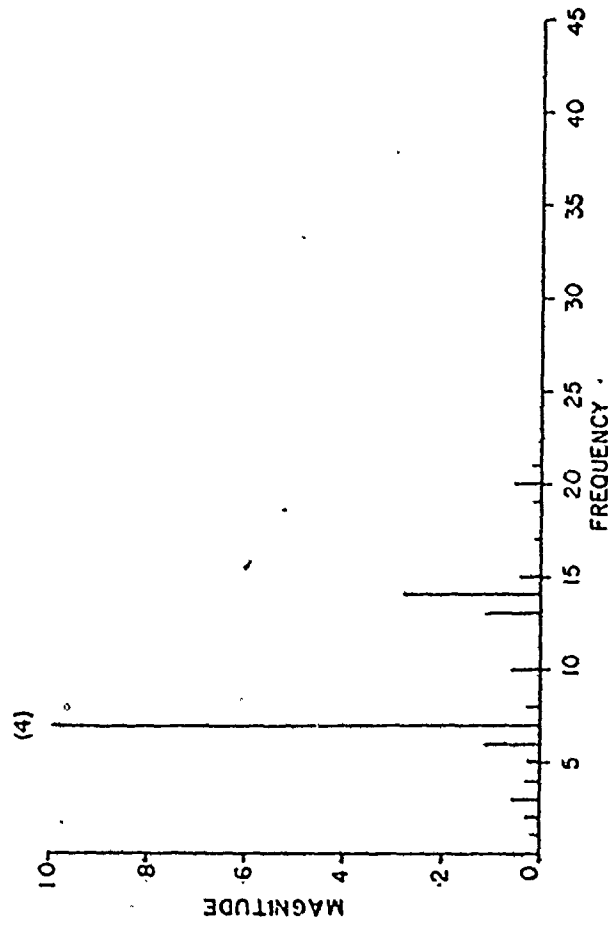


Fig 3.7: Power Spectral Density of the Pyloric Mechanical activity- 10 minutes after feeding.

POWER SPECTRUM- DUODENAL MECHANICAL
ACTIVITY(10min)

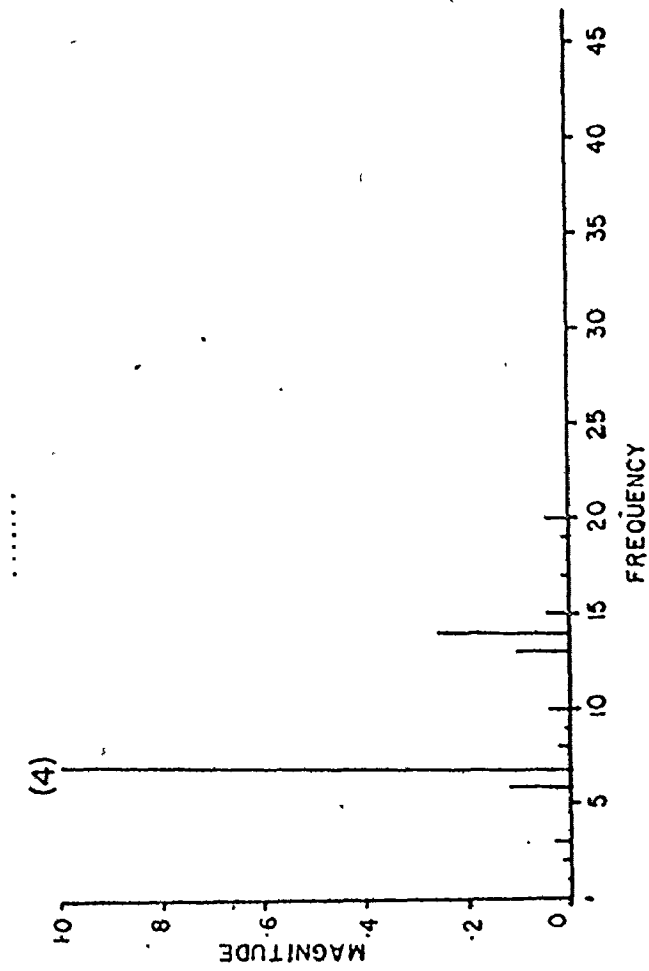


Fig 3.8: Power Spectral Density of the Duodenal Mechanical activity- 10 minutes after feeding.

GASTROJUDENAL ELECTRICAL & MECHANICAL
ACTIVITIES (Pentagastrin - 4 Minutes)

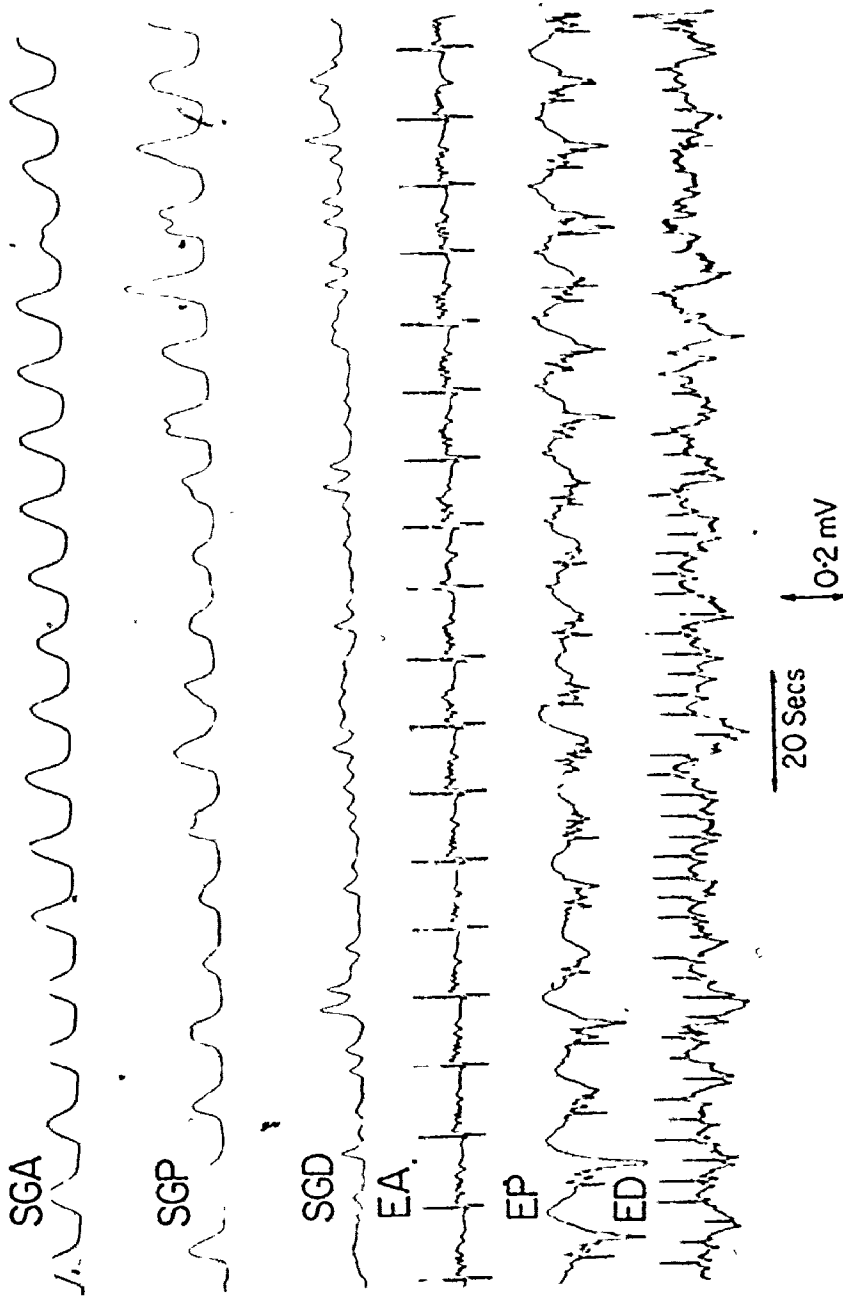


Fig 3.9: Electrical and Mechanical activities recorded
from a dog. (4 minutes after Pentagastrin)

POWER SPECTRUM- PYLORIC ELECTRICAL
ACTIVITY (Pentagastrin -4 Minutes)

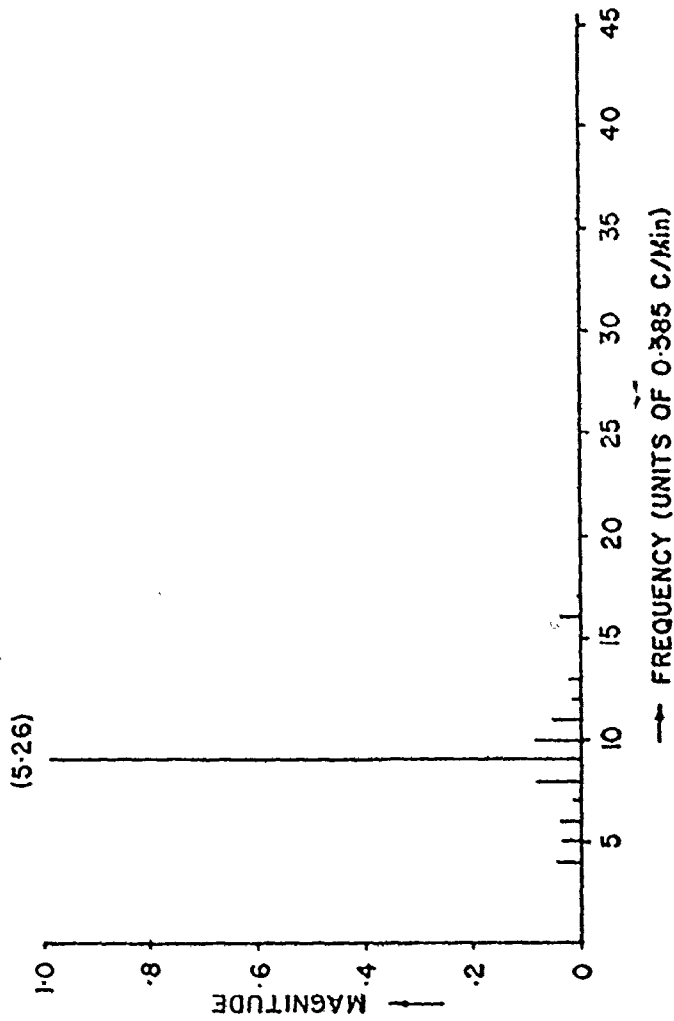


Fig 3.10: Power Spectral Density of the Pyloric Electrical activity- 4 minutes after Pentagastrin infusion.

POWER SPECTRUM - DUODENAL ELECTRICAL
ACTIVITY (Pentagastrin - 4 Minutes)

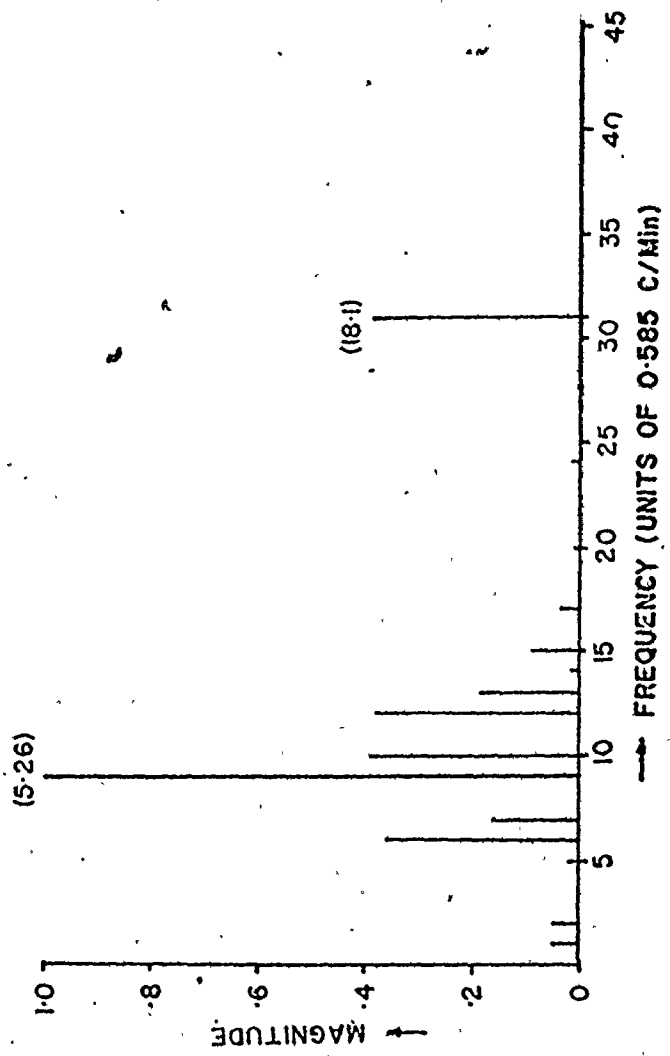


Fig 3.11: Power Spectral Density of the Duodenal Electrical activity- 4 minutes after Pentagastrin infusion.

POWER SPECTRUM - PYLORIC MECHANICAL
ACTIVITY (Pentagastrin-4 Minutes)

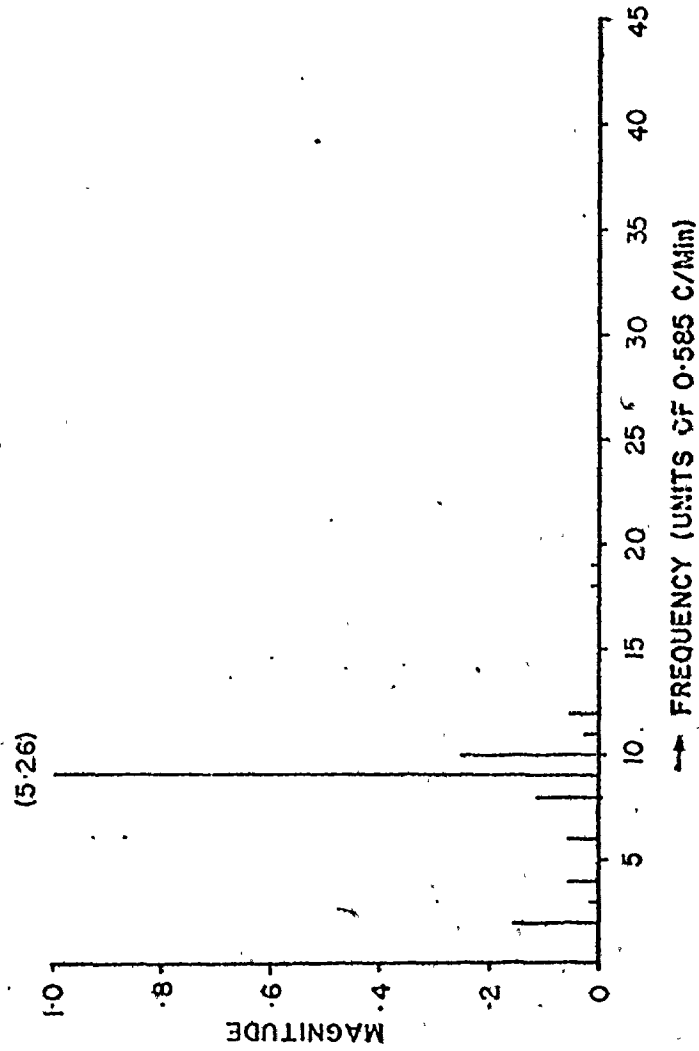


Fig 3.12: Power Spectral Density of the Pyloric Mechanical activity- 4 minutes after Pentagastrin infusion.

POWER SPECTRUM - DUODENAL MECHANICAL ACTIVITY (Pentagastrin - 4 Minutes)

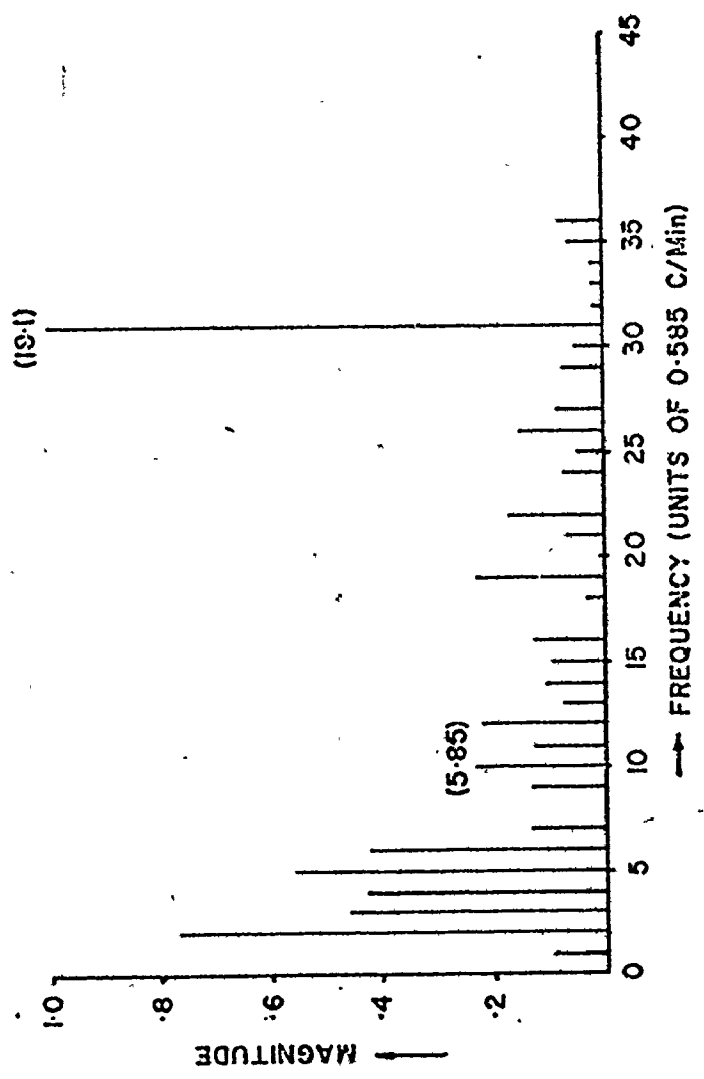


Fig 3.13: Power Spectral Density of the Duodenal Mechanical activity- 4 minutes after Pentagastrin infusion.

GASTRODUODENAL ELECTRICAL &
MECHANICAL ACTIVITIES (Atropine)

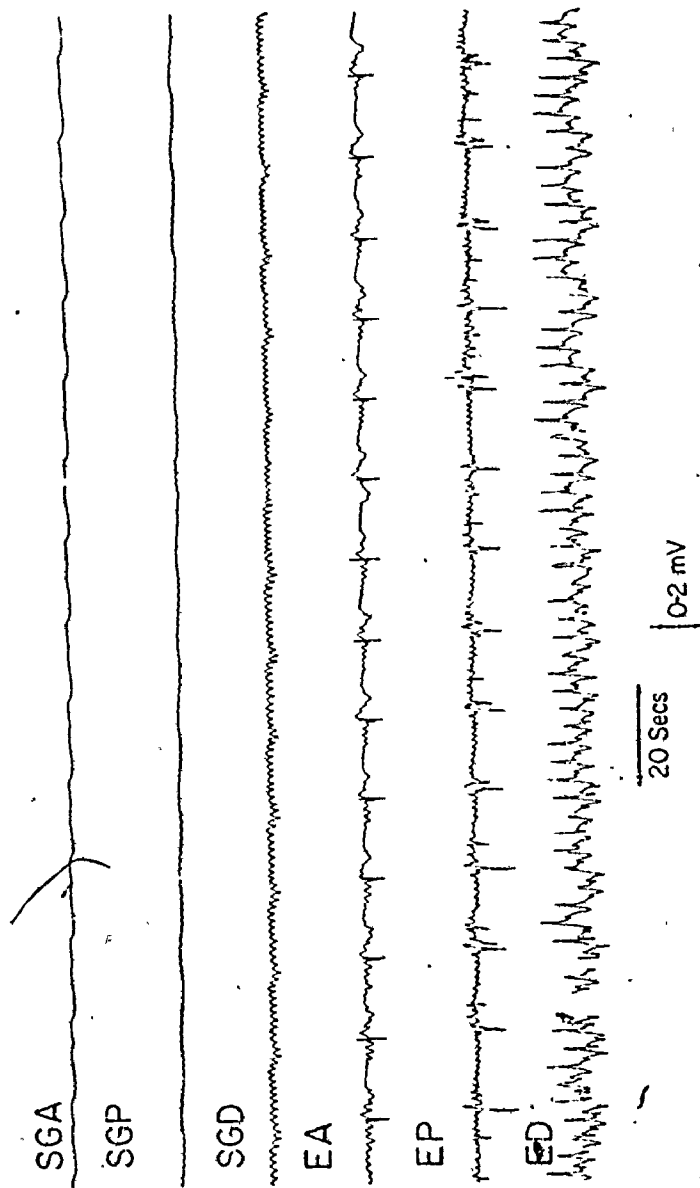


Fig 3.14: Electrical and Mechanical activities recorded
from a dog. (after Atropine)

POWER SPECTRUM-DUODENAL ELECTRICAL
ACTIVITY (Atropine)

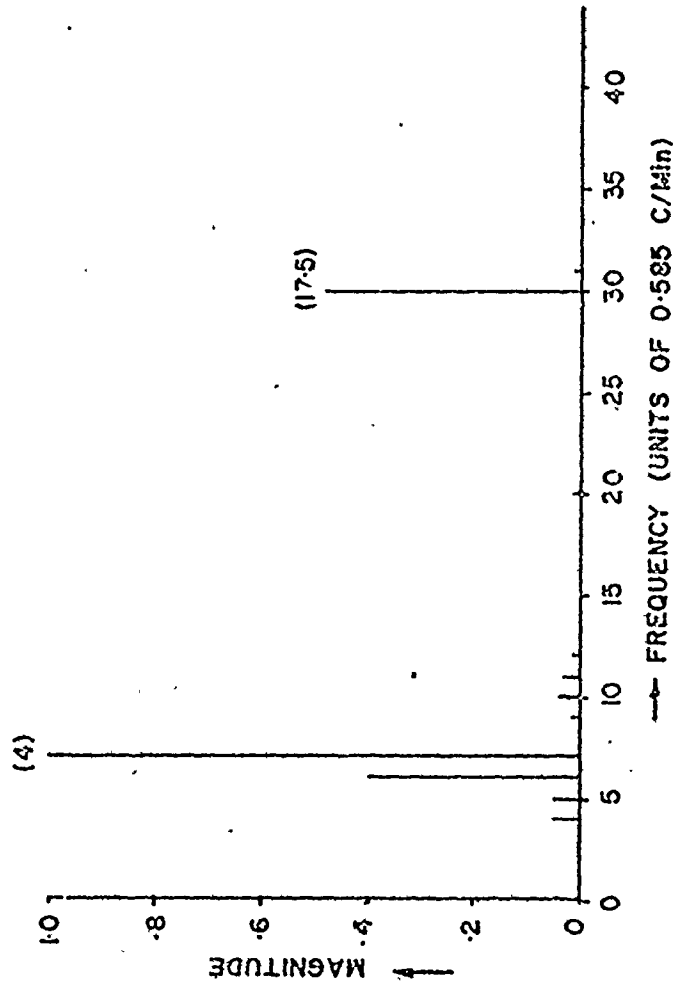


Fig 3.15: Power Spectral Density of the Duodenal Electrical activity- after Atropine.

Table 3.1: Dog No. 1 - Experiments with food

Expt No	Fasted state	15 minutes after food	30 minutes after food	45 minutes after food	minutes after food	After Atropine
	A B C D E	A B C D E	A B C D E	A B C D E	A B C D E	A B C D E
1	X X X X X	X X X X X	X X X X X	- - X X -	-	
2	X X - - X	X X X X X	X X X X X	- - - -		

Comments: The magnitude of antral frequency component in the duodenal electrical activity is small when present and is absent sometimes. The duodenal mechanical activity shows increased antral frequency component after food. The lower cut off frequency used in recording was .16 Hz, different from other experiments (5.3 Hz)

Table 3.2: Dog No. 2 - Experiments with food																				
Expt No	Fasted state					15 minutes after food		30 minutes after food		45 minutes after food		60 minutes after food		After Atropine						
	A	B	C	D	E	A	B	C	D	E	A	B	C	D	E	A	B	C	D	E
1	X	X	-	-	X	X	X	-	-	X	X	X	-	-	X	-	-	-	-	-
2	X	X	-	-	X	X	-	-	X	X	X	X	-	-	X	-	-	-	-	-
3	X	X	-	-	X	X	X	-	-	X	X	X	-	-	X	X	X	-	-	X
4	-	X	-	-	X	X	X	-	-	X	X	X	-	-	X	-	-	-	-	-
5	-	-	-	-	X	X	X	-	-	X	X	X	-	-	X	-	-	-	-	-

Comments: The magnitude of PSD at antral frequency in the pyloric electrical activity is small when compared to duodenal frequency component. This leads to doubt about the location of the electrode. The magnitude of PSD at antral frequency in the duodenal electrical and mechanical activity increases after food

Table 3.3: Dog No. 3 - Experiments with food

Expt No	Fasted state					15 minutes after food					30 minutes after food					45 minutes after food					minutes after food					After Atropine									
	A	B	C	D	E	A	B	C	D	E	A	B	C	D	E	A	B	C	D	E	A	B	C	D	E	A	B	C	D	E					
1	X	X	-	-	X	X	X	-	-	X	X	X	-	-	X	X	X	-	-	X	X	X	-	-	X										
2	X	X	-	-	X	X	X	-	-	X	X	X	-	-	X	X	X	-	-	X	X	X	-	-	X										
3	X	X	-	-	X	-	-	-	-	-	X	X	-	-	X	X	X	-	-	X	X	X	-	-	X										
4	X	X	-	-	X	X	X	-	-	X	X	X	-	-	X	X	X	-	-	X	X	X	-	-	X										
5	X	X	-	-	X	X	X	-	-	X	X	X	-	-	X	X	X	-	-	X	X	X	-	-	X										

Comments: The duodenal frequency component in the pyloric electrical activity is absent sometimes and very low if present. The antral frequency component in the duodenal electrical and mechanical activity increases after food

Table 3.4: Dog No. 4 - Experiments with food

Expt No	Fasted state					15 minutes after food					30 minutes after food					45 minutes after food					minutes after food					After Atropine									
	A	B	C	D	E	A	B	C	D	E	A	B	C	D	E	A	B	C	D	E	A	B	C	D	E	A	B	C	D	E					
1	X	X	-	-	-	X	X	X	X	X	X	X	X	X	X	X	X	X	X	X	X	X	X	X	X										
2	X	X	-	-	X	X	X	X	X	X	X	X	X	X	X	X	X	X	X	X	X	X	X	X	X										
3	-	-	-	-	-	-	-	-	-	-	X	X	X	X	X	X	X	X	X	X	X	X	X	X	X										
4	X	X	-	-	-	X	X	X	X	X	X	X	X	X	X	X	X	X	X	X	X	X	X	X	X										
5	X	X	-	-	X	X	X	X	X	X	X	X	X	X	X	X	X	X	X	X	X	X	X	X	X										
6.	Y	X	-	-	X	X	X	-	-	X	X	X	-	-	X	X	X	-	-	X	X	X	-	-	X										

Comments: The duodenal frequency component in the pyloric electrical activity is absent sometimes and is low when present. The antral frequency component magnitude in the duodenal electrical and mechanical activity increases after food

Table 3.5: Dcg No. 5 - Experiments with food

Expt No	Fasted state					15 minutes after food					30 minutes after food					45 minutes after food					minutes after food					After Atropine					
	A	B	C	D	E	A	B	C	D	E	A	B	C	D	E	A	B	C	D	E	A	B	C	D	E	A	B	C	D	E	
1	X	X	-	-	-	X	X	-	-	-	X	X	-	-	-	X	X	X	-	-	X	-	-	-	-	-	-	-	-	-	-
2	-	-	-	-	-	X	X	-	-	-	X	X	-	-	-	X	X	-	-	-	-	-	-	-	-	-	-	-	-	-	
3	X	X	-	-	X	X	X	X	X	X	X	X	X	X	X	X	X	X	X	X	-	-	-	-	-	X	X	-	-	-	
4	X	X	-	-	X	X	X	X	X	X	X	X	X	X	X	X	X	X	X	X	-	-	-	-	-	-	-	-	-	-	
5	X	X	-	-	-	X	X	X	X	X	X	X	X	X	X	X	X	X	X	X	-	-	-	-	-	-	-	-	-	-	
6	X	X	-	-	-	X	X	X	X	X	X	X	X	X	X	X	X	X	X	X	-	-	-	-	-	-	-	-	-	-	

Comments: The duodenal frequency component in the pyloric electrical activity is absent sometimes and low when present. The antral frequency component in the duodenal electrical and mechanical activity increases after food

Table 3.6: Dog No. 1 - Experiments with Pentagastrin

Expt No	Fasted state	15 min. after Pentagastrin	30 min. after Pentagastrin	45 min after Pentagastrin	min. after Pentagastrin	After Atropine
	A B C D E	A B C D E	A B C D E	A B C D E	A B C D E	A B C D E
1	X X - - X	X X - - -	X X - - X			
2	- - - - -	X X - - X	X X - - X			

Comments: The magnitude of PSD at the duodenal frequency in the pyloric electrical activity is small and absent sometimes. The antral frequency component in the duodenal electrical activity was small. The lower cut off frequency used in recording was .16 Hz, different from other experiments (5.3 Hz)

Table 3.7: Dog No. 2 - Experiments with Pentagastrin

Expt No	Fasted state					15 min. after Pentagastrin					30 min. after Pentagastrin					45 min. after Pentagastrin					min. after Pentagastrin					After Atropine				
	A	B	C	D	E	A	B	C	D	E	A	B	C	D	E	A	B	C	D	E	A	B	C	D	E	A	B	C	D	E
1	X	X	-	-	X	X	X	-	-	X	X	X	-	-	X	X	X	-	-	X	-	-	-	-	-	-	-	-	-	-
2	X	X	-	-	X	X	X	-	-	X	X	X	-	-	X	X	X	-	-	X	-	-	-	-	-	-	-	-	-	-
3	X	-	-	-	X	X	X	-	-	X	X	X	-	-	X	X	X	-	-	X	-	-	-	-	-	-	-	-	-	-
4	-	-	-	-	-	X	X	-	-	X	X	X	-	-	X	X	X	-	-	X	-	-	-	-	-	-	-	-	-	-
5	X	-	-	-	X	X	-	-	-	X	X	X	-	-	X	-	-	-	-	-	-	-	-	-	-	X	-	-	-	X

Comments: The magnitude of PSD at antral frequency in electrical activity is absent in some cases and very small compared to duodenal frequency. It is suspected that pylorus electrode is very close to the duodenum

Table 3.8: Dog No. 4 - Experiments with Pentagastrin																														
Expt No.	Fasted state		15 min. after Pentagastrin					30 min. after Pentagastrin					45 min. after Pentagastrin					min after Pentagastrin					After Atropine							
	A	B	C	D	E	A	B	C	D	E	A	B	C	D	E	A	B	C	D	E	A	B	C	D	E	A	B	C	D	E
1	X	X	-	-	X	X	X	Y	X	X	X	X	X	X	X	X	X	X	X	X	X	X	X	X	X	X	X	X	X	X
2	X	X	-	-	-	X	X	X	X	X	X	X	X	X	X	X	X	X	X	X	X	X	X	X	X	X	X	X	X	X
3	-	-	-	-	-	X	X	-	-	X	X	X	-	-	X	X	X	-	-	X	X	X	-	-	X	X	X	-	-	X
4	X	X	-	-	X	X	X	-	-	X	X	X	-	-	X	X	X	-	-	X	X	X	-	-	X	X	X	-	-	X
5	-	-	-	-	-	X	X	X	-	-	X	X	-	-	X	X	X	-	-	X	X	X	-	-	X	X	X	-	-	X

Comments: The duodenal frequency component in the pyloric electrical activity is absent some times and is low in magnitude when present. The antral frequency component in the duodenal electrical activity with pentagastrin is higher than in the fasted state and when Atropine was given.

Expt No		Table 3.9: Dog No. 5 - Experiments with Pentagastrin																																		
		Fasted state					15 min. after Pentagastrin					30 min. after Pentagastrin					45 min. after Pentagastrin					min after Pentagastrin					After Atropine									
		A	B	C	D	E	A	B	C	D	E	A	B	C	D	E	A	B	C	D	E	A	B	C	D	E	A	B	C	D	E					
1		X	X	-	-	X	X	X	X	X	X	X	X	X	X	X	X	X	X	X	X	-	-	-	-	-	-	-	-	-	-	X	X	-	-	-
2		X	X	-	-	X	X	X	X	-	-	-	-	-	-	-	-	-	-	-	-	-	-	-	-	-	-	-	-	-	-	X	X	-	-	X
3		X	X	-	-	X	X	X	X	-	-	X	X	X	-	-	X	X	X	-	-	-	-	-	-	-	-	-	-	-	-	X	X	-	-	-
4		X	X	-	-	X	X	X	X	X	-	X	X	X	X	-	-	-	-	-	-	-	-	-	-	-	-	-	-	-	-	X	X	-	-	X
5		X	X	-	-	X	X	X	X	X	X	X	X	X	X	X	X	X	X	X	X	-	-	-	-	-	-	-	-	-	-	X	X	-	-	-
6		X	X	-	-	X	X	X	X	X	X	-	-	-	-	-	-	-	-	-	-	-	-	-	-	-	-	-	-	-	-	X	X	-	-	X

Comments: The magnitude of PSD at antral frequency in the duodenal electrical activity increases with pentagastrin. It is low in fasted state and with Atropine. The magnitude of PSD at the duodenal frequency in the electrical activity of the pylorus is small, if present and absent some times

4. CONCLUSIONS

The electrical and mechanical signals recorded from the gastroduodenal junction of 5 dogs were analysed on the Mini-computer. The programs developed compute the power spectra of signals with a frequency resolution of 0.585 c/min. The power spectra of a given stretch of data of about 100 secs duration show frequency components of significance along with spurious components. The spurious frequency components can be attributed to randomness of wave shape. If it is desired to avoid the spurious components in the spectra, the source data can be filtered with a band pass filter before frequency analysis.

Analysis of the pyloric and duodenal electrical activities in 5 dogs reveals the following characteristics.

* A. The pyloric electrical activity shows a stronger component at 4.-4.68 c/min both in the fasted state and when food is present in the stomach. The magnitude of PSD at the duodenal frequency is usually very low and sometimes absent.

B. The duodenal electrical activity shows the antral and duodenal frequency components both in the fasted and fed states. The magnitude of PSD in the recordings at the antral frequency in comparison with that at the duodenal frequency increased after food.

Similar effects were observed with Pentagastrin infusion at 4 ug/kg/hr. Pentagastrin also increased the antral and the duodenal ECA

frequencies to 5.49 ± 0.1 (SE) c/min and $19.18 \pm .53$ (SE) c/min respectively. The antral and the duodenal frequencies before pentagastrin was 4.35 ± 0.2 (SE) c/min and 18.1 ± 0.30 (SE) respectively.

These results support the observation made by Allen, Poole and Code [8], McCoy and Bass [9] and E. Atannasova [7] in that a correlation exists between the electrical response activities recorded from the distal antrum and the proximal duodenum of dogs. Though others reported coordination, their results were based on visual analysis and were subjective. Only the good records were analysed. The present study was carried out by analysing signals in the fasted state and 15, 30, and 45 minutes after food and pentagastrin infusion in most of the cases. The computer methods facilitate the analysis of signals, even when they are complex and corrupted by random fluctuations.


The pylorus does not act as an electrical insulator as concluded by Bass, Code and Lambert [6]. The signals recorded in the pylorus in the present work exhibit mainly antral frequency components.

Visual examination of the records shows that there is a phase lag between the occurrence of the response activity in the antrum and the pylorus. This suggests that the contractions in the distal antrum do not occur simultaneously. The pylorus can, therefore, be considered as an extension of the antrum because it contracts largely at the antral rate.

Analysis of the pyloric and the duodenal mechanical activities reveals the following characteristics.

A. The pyloric mechanical activity indicates a frequency component at the control frequency (4 - 4.68 c/min). No duodenal frequency com-

ponent was present. After pentagastrin infusion, the frequency increased 5.25 - 5.85 c/min. In the fasted state, the pyloric contractions were absent most of the time.



B. The duodenal mechanical activity shows both antral and duodenal frequency components after food and pentagastrin infusion. With pentagastrin, the antral frequency component in comparison with duodenal frequency component is not as strong as it is after feeding. The reason for this difference may be due to the fact that Pentagastrin would not stimulate all the nerves that become active and coordinate mechanical activity after feeding.

These results imply that after a meal, antral contraction reaches the pylorus and often ends in a contraction of the pylorus and the proximal duodenum. In other words, the antrum and the duodenum work as a coordinated unit. This conclusion is in agreement with that reported by Papazova, Atanassova and Rodeva [7].

There are three possible mechanisms of coordination. They are: a) the myogenic mechanism which is due to the coupling and interaction of the antral and the duodenal relaxation oscillators, b) the neurogenic mechanism - in this case the nerves that enter the gastric wall may cross over to the duodenum. When food is present in the stomach, they may inhibit the normal duodenal contractions, c) the mechanical stimulation - initiation of contraction by the chyme emptied by the antrum.

Analysis of the records after atropine was given reveals the antral component in the electrical activities of the pylorus and the duodenum. [Atropine blocks the action of nerves that cause contrac-

tions.] This suggests that myogenic interaction across the gastro-duodenal junctions exists.

The phase lag information at antral frequency in the pyloric and the duodenal electrical and mechanical activities was obtained by computing the phase of the cross spectra. Lag time computed from this angle is dependent on the wave shape of signals. If signals are of different wave shape, time lag computed will not represent the delay between the occurrence of ECA or mechanical contraction at the two sites. In the present study, the main emphasis is on the spread of antral waves into the proximal duodenum. To determine the time lag at the antral frequency, the source data can be filtered by a bandpass filter (passband suggested is 3-6 c/min) and cross spectral analysis can be carried out on the filtered data. The time lag information obtained may possibly be useful in determining the precise mechanism of coordination.

BIBLIOGRAPHY

1. S.K. Sarna, "A Feedback loop to control Gastric emptying", Digest of the 11th International Conference and Biological Engineering, August 1976, Ottawa.
2. S.K. Sarna, "Gastro intestinal Electrical Activity: Terminology", Gastroenterology, 68, pp. 1631-1635, The Williams and Wilkins Co., 1975.
3. S.K. Sarna, E.E. Daniel and Y.J. Kingma, "Simulation of the Electrical-Control Activity of the Stomach by an Array of Relaxation Oscillators", Digestive Diseases, Vol. 17, No. 4, April 1972.
4. D.A.W. Edwards and E.N. Rowlands, "Physiology of the gastroduodenal junction", Handbook of Physiology, Sec. 6, Vol. IV, American Physiological Society, 1968.
5. Alvarez and J. Mohoney, "Relations between gastric and Duodenal Peristalsis", The American Journal of Physiology, pp. 376-385, vol. 64, 1923.
6. P. Bass, F. Code and E.H. Lambert, "Electric Activity of gastroduodenal junction", The American Journal of Physiology, Vol. 2, October 1961.
7. E. Atanassova, "Bio-electrical activity of stomach and Duodenum after cutting the gastroduodenal function", Bulletin of the Institute of Physiology, TOM (Vol.) XIII, 1970.

8. Allen C.L., E.W. Poole and C.F. Code, "Relationship between electrical activities of antrum and duodenum", American Journal of Physiology
9. E.J. McCoy and P. Bass, "Chronic electrical activity of gastroduodenal area: effects of food and certain catechola mines", American Journal of Physiology, Vol. 3, 1963.
10. Bortoff and R.S. Davis, "Myogenic transmission of antral slow waves across the gastroduodenal junction in situ", American Journal of Physiology, No. 4, October 1968.
11. P. Bass and J.N. Wiley, "Contractile force transducer for recording muscle activity in unanesthetized animals", Journal of Applied Physiology, Vol. 12, No. 4, April 1972.
12. L.E. Franks, "Signal Theory", Prentice Hall, International, 1969.
13. William English, "How to use the NOVA computers", Data General Corporation, Massachusetts
14. K. Muniappan, "Computer analysis of Gastroduodenal electrical and mechanical activities", Report No. GIR-1, Bio-medical Group, Department of Electrical Engineering, McMaster University, Canada.
15. Tektronix, "4010 and 4010-1 User's Manual", Tektronix Inc., P.O. Box 500, Beaverton.
16. Robert K. Otneg and Loren Enochson, "Digital Time Series Analysis", pp. 273, Wiley Inter. Science, 1972.
17. Schwartz and Shaw, "Signal Processing: Discrete Spectral Analysis, Detection and Estimation", pp. 159-190, McGraw Hill Book Company, 1975.

18. Schwartz and Shaw, "Signal Processing: Discrete Spectral Analysis, Detection and Estimation", pp. 91-93, McGraw Hill Book Company, 1975.
19. B. Gold and C. Rader, "Digital Processing of Signals", McGraw-Hill Book Company, 1969.
20. Alan V. Oppenheim and Ronald W. Schaffer, "Digital Signal Processing", pp. 332, Prentice-Hall Inc., 1975.
21. Bendat and Piersal, "Measurement and Analysis of Random Data", pp. 14, John Wiley and Sons Inc.
22. D.A. Linkens and A.E. Cannell, "Interactive Graphics Analysis of Gastrointestinal Electrical Signals", IEEE Transactions on Biomedical Engineering, pp. 335-339, July 1974.
23. D.A. Linkens and Z.B. Temel, "The use of Walsh Transform in the Analysis of Gastrointestinal Signals", unpublished note from the Department of Control Engineering, University of Sheffield, England.